

# Hydration of the 222 Cryptand and 222 Cryptates Studied by Molecular Dynamics Simulations<sup>†</sup>

P. Auffinger and G. Wipff\*

Contribution from the Institut de Chimie, 1 rue Blaise Pascal, 67000 Strasbourg, France.  
Received August 13, 1990

**Abstract:** Solvent effects and structure of ionophores in solution are felt to be essential for determining their binding selectivity, solubility, or transport capability, but these are generally not precisely known. We report here a theoretical study, using molecular dynamics simulations, on a prototypical system: the bicyclic 222 cryptand in water, either in its free state or with complexed cations (from Li<sup>+</sup> to Cs<sup>+</sup>, Ca<sup>2+</sup>, and Eu<sup>3+</sup>) with explicit representation of the solvent. It is found that the uncomplexed 222, which is neither conformationally organized in the solid state nor in the gas phase for cation complexation, adopts in water preferentially a conformation suitable for ionophoric behavior. This conformer, which presents a cavity with converging binding sites and a diverging "hydrophobic skin", has no water inside. It is stabilized by three interbridging water molecules forming an arrangement of C<sub>3</sub> symmetry. Alternative forms, in which nitrogen or oxygen binding sites are diverging and more accessible to the solvent, are less well hydrated. We suggest that "solvent-induced preorganization" can occur in other macro(poly)cyclic systems with gauche XC-CX (X = N, O) arrangements of suitable topology. For the cation complexes, we investigate the effectiveness of solvent shielding by the ionophore for encapsulated cations of increasing size (from Li<sup>+</sup> to Cs<sup>+</sup>) or charge (in the Na<sup>+</sup>, Ca<sup>2+</sup>, Eu<sup>3+</sup> series). There are both direct cation-water coordination and longer range cation-water interactions of increasing importance as the cationic charge increases. Particularly, the coordination number of Eu<sup>3+</sup> calculated for the Eu<sup>3+</sup>/222 cryptate (3.9) agrees well with experimental values. This microscopic description of the hydration pattern allows for reinterpretation of several experimental results and provides deeper insights into dynamical features and solvation effects on molecular recognition.

## Introduction

Although the precise structure and conformation of macro(poly)cyclic receptors such as crown ethers, cryptands, and podands are felt to be essential for controlling their ionophoric properties, very little is known about them in the conditions where complexation and transport take place, i.e., in solution. It has been shown, mostly on the basis of solid-state structures,<sup>1</sup> that organization of their binding sites around the potential substrate is a key factor controlling the binding ability and selectivity.<sup>2,3</sup> Structures *in solution* are assumed to be similar, as far as the inclusive nature of the complexes involving converging binding sites is concerned, but except for conformationally preorganized rigid systems,<sup>3</sup> the precise conformation is unknown since it cannot be determined by techniques like NMR (because of rapid conformational equilibria). More generally, detailed knowledge of structures *in solution* and of solvation patterns is essential to understand the basis of molecular recognition.

Forming "lock and key" arrangements between the receptor and the substrates may not be a simple intrinsic feature of the partners, since solution and environmental effects play a significant role. The solvent affects not only the complex stabilities and selectivities<sup>4</sup> but also the nature of the complex. For example, depending on the nature of the solvent and of the counterion, 222/Cs<sup>+</sup> cryptates may be of the "inclusive" or "exclusive" type,<sup>5</sup> although in the solid state Cs<sup>+</sup> sits at the center of the cage.<sup>1</sup> A more dramatic example is provided by a NO<sub>3</sub><sup>-</sup> cryptate: In water, an inclusive complex of 1:1 stoichiometry is formed, but in the solid-state structure, NO<sub>3</sub><sup>-</sup> is *outside*, rather than *inside*, the cage.<sup>6,7</sup> It has been recently suggested that the binding mode of carboxylate derivatives to cyclodextrins differs in water from that in *N,N*-dimethylformamide.<sup>8</sup> It is stressed, although difficult to prove experimentally, that conformations of crown ethers and of uncomplexed macrocyclic receptors are solvent dependent.<sup>9,10</sup> Water as a solvent may give rise to particular interactions, not only in solvating charged species, but also by interacting with neutral ionophores in their free state, a question that, as quoted recently, has not yet received appropriate attention.<sup>11</sup>

In this study, we analyze several aspects of hydration relevant for molecular recognition in general. First, we address the question of the solvent effect on the conformation of the free receptor: Does it stabilize several conformers equally well? If not, how does the

solid-state structure, characterized for the free receptor, behave in water? Does solvation favor conformations that are preorganized for complexation (i.e., having a cavity with converging binding sites) more than structures unsuitable for complexation (i.e., without cavity or with diverging binding sites)? Do solvent molecules take the place of potential substrates inside the receptor's cavity? How does the solvation energy correlate with the surface of heteroatoms accessible to the solvent? In order to act as a cation carrier through hydrophobic membranes, the receptor has to shield this encapsulated cation from the environment and to present as much as possible a hydrophobic "skin". How efficient is that shielding in the aqueous phase and in the organic phase?

In order to gain insight into these basic questions, we used molecular dynamics simulations for a prototypical carrier, the bicyclic 222 cryptand free and complexed in water. It was the first synthetic cage compound<sup>12-14</sup> to complex with high stability and selectivity spherical cations such as K<sup>+</sup> and to transport them through liquid membranes.<sup>15</sup> 222 is a good candidate for theoretical studies because of the amount of experimental studies and the many structural<sup>1</sup> and thermodynamic data<sup>4</sup> available. Compared to 18-crown-6, which has been subjected to many simula-

(1) Döbler, M. *Ionophores and their Structures*; Wiley Interscience: New York, 1981.

(2) Lehn, J. M. *Angew. Chem., Int. Ed. Engl.* **1988**, *27*, 89-112.

(3) Cram, D. J. *Science* **1988**, *240*, 760-767.

(4) Izatt, R. M.; Bradshaw, J. S.; Nielsen, S. A.; Lamb, J. D.; Christensen, J. J.; Sen, D. *Chem. Rev.* **1985**, *85*, 271-339.

(5) Kauffmann, E.; Dye, J. L.; Lehn, J. M.; Popov, A. I. *J. Am. Chem. Soc.* **1980**, *102*, 2274-2276.

(6) Heyer, D.; Lehn, J. M. *Tetrahedron Lett.* **1986**, *27*, 5869-5872. Rubin, C. Thèse de Pharmacie, Université de Nancy, France, 1991.

(7) Pascard, C.; Lehn, J. M. Unpublished results, 1986.

(8) Danil de Namor, A. F.; Traboulsi, R.; Lewis, D. F. V. *J. Chem. Soc., Chem. Commun.* **1990**, 751-753.

(9) Mosier-Boss, P. A.; Popov, A. I. *J. Am. Chem. Soc.* **1985**, *107*, 6168-6174.

(10) Schmidt, E.; Tremillon, J. M.; Kintzinger, J. P.; Popov, A. I. *J. Am. Chem. Soc.* **1983**, *105*, 7563-7566.

(11) Olsher, U.; Frolow, F.; Bartsche, R. A.; Pugia, M. J.; Shoham, G. *J. Am. Chem. Soc.* **1989**, *111*, 9217-9222.

(12) Dietrich, B.; Lehn, J. M.; Sauvage, J. P.; Blanzat, J. *Tetrahedron* **1973**, *29*, 1629-1645.

(13) Dietrich, B.; Lehn, J. M.; Sauvage, J. P. *Tetrahedron* **1973**, *29*, 1647-1658.

(14) Lehn, J. M. *Acc. Chem. Res.* **1978**, *11*, 49-57.

(15) Behr, J. P.; Kirch, M.; Lehn, J. M. *J. Am. Chem. Soc.* **1985**, *107*, 241-246.

<sup>†</sup> Key words: 222 cryptand and cryptates; ionophores; hydration; molecular dynamics; molecular modeling; molecular recognition; preorganization.

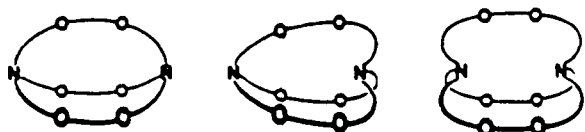


Figure 1. *out-out*, *out-in*, and *in-in* topomers of the 222 bicyclic cryptand.

tions in the gas phase<sup>16,17</sup> and in solution,<sup>18–21</sup> bicyclic cryptands like 222 lead to cation complexes of higher stability and selectivity<sup>4</sup> and to more efficient transport.<sup>15</sup> In addition, 222 represents a class of neutral ionophores, which might display specific interactions with water, as compared to charged ionophores. We report here the first simulations on this receptor *in water* in its free state (cryptand), as well as in its cation complexes (cryptates). For the cryptand, we compare several conformations extracted from solid-state structures that are relevant for the discussion of *preorganization* and *ionophoric behavior*. Subsequently a variety of cryptates are considered in order to assess the effects of the cationic size (from  $\text{Li}^+$  to  $\text{Cs}^+$ ) and charge (in the  $\text{Na}^+$ ,  $\text{Ca}^{2+}$ ,  $\text{Eu}^{3+}$  series) on their dynamical behavior and on the cation/receptor complementarity. We compare also their hydration pattern and analyze particularly to what extent the encapsulated cation is shielded from the solvent by the 222 ligand.

There have been molecular mechanics,<sup>22,23</sup> molecular dynamics, and normal mode analysis<sup>24</sup> on X-ray and model-built structures of 222 in the gas phase, in its free form as well as for cation complexes. Recently, the hydration of *in-in* and *out-out* conformers of protonated 222,  $\text{H}^+$  and 222,  $2\text{H}^+$  forms has been simulated by molecular dynamics.<sup>120</sup> We performed also free energy perturbation calculations on the  $\text{Na}^+$ ,  $\text{K}^+$ , and  $\text{Rb}^+$  binding selectivity of 222 in water and in methanol.<sup>121</sup> A search of the conformational space of 222 neutral using "high temperature annealed molecular dynamics simulations" led to the conclusion that the uncomplexed form is not in the gas phase, conformationally preorganized for cation complexation.<sup>25</sup> The most stable forms were quite elongated, without converging binding sites delineating a "spherical" cavity, essentially because of electrostatic repulsions between the C–O or C–N dipoles. None of the known cryptate-type conformers was produced for the free cage. A trend was found for decreasing stabilities going from *in-in*, to *in-out*, and *out-out* orientations of the nitrogen lone pairs (Figure 1), but the energy gap was small (less than 5 kcal/mol) and we proposed a leveling out of these forms in protic solvents. It was shown that  $\text{K}^+$ , the alkali cation that displays the best complementarity with 222, induces the conformation found in solid-state structures for the  $\text{K}^+$  cryptate. From these gas-phase results,<sup>25</sup> it was suggested that the average  $D_3$  form observed by NMR for 222 uncomplexed in solution<sup>12</sup> might result from a contribution of a large number of asymmetrical conformers<sup>25</sup> rather than from a few symmetrical conformers. The results reported here show that hydration effects lead to conclusions different from those drawn from gas-phase studies.

Although MD simulations are in principle able to sample the conformational space, they explore, in fact at 300 K within 50 ps, a very restricted part of this conformational space around the

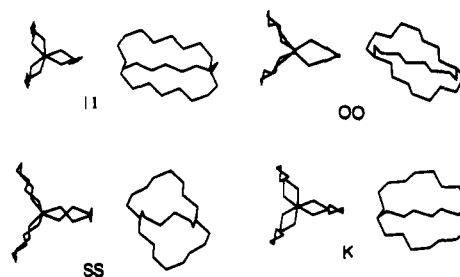


Figure 2. II, OO, SS, and K conformers of the 222 cryptand (orthogonal views).

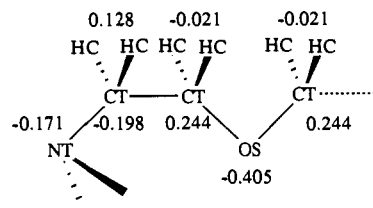


Figure 3. Charges for the  $-\text{NCH}_2\text{CH}_2\text{OCH}_2-$  moiety of 222.

starting conformer. "Hunting for the global minimum", a problem generally addressed by gas-phase simulations,<sup>26,27</sup> is a very challenging problem in solution. The longest MD simulation reported so far on a macrocyclic compound in water, 18-crown-6,<sup>19</sup> showed that, during 1.5 ns, many new conformations were produced, without convergence. Given computer time limitations, we restrict the study of 222 uncomplexed in water to four typical conformations derived from X-ray structures, rather than seeking for "the" most stable form in solution. They will be referred to later as II, OO, SS, and K, consistently with the notation used previously<sup>25</sup> (Figure 2). They were selected for the following reasons. The II conformer (II stands for "In-In") is calculated to be close to the energy minimum in vacuo<sup>22,23,25</sup> and corresponds to 222 uncomplexed in the solid state. It is quite elongated, without a cavity. Of these conformers, only K is of cryptate type. (The notation K is to remember that it is taken from the  $\text{K}^+$  cryptate and displays therefore a spherical cavity complementary to  $\text{K}^+$ , the alkali cation that is the best "recognized" by 222<sup>13</sup>). However, because most of the solvent accessible surface is formed by hydrophobic  $\text{CH}_2$  groups, the K form might be anticipated to be poorly hydrated and weakly populated in water. The OO and SS forms have instead diverging nitrogen or oxygen binding sites. The OO form (OO stands for "Out-Out") is extracted from the bis- $(\text{BH}_3)$  molecular adduct of 222, and SS is taken from a dithia analogue of 222, in which the sulfur atoms are replaced by oxygen atoms.<sup>28</sup> If the hydration energy is proportional to the solvent accessible surface of the heteroatoms (17, 14, 25 and 8 Å<sup>2</sup>, respectively for II, OO, SS, and K<sup>25</sup>), one would predict SS to be the best and K the worst hydrated among these forms. The results reported here show that this is not so.

### Computational Procedure

Molecular dynamics calculations were performed with the program AMBER 3.0,<sup>29</sup> by using the representation of the potential energy given in ref 30.

The bonds and bond angles are treated as harmonic springs, and a torsional term is associated with the dihedral angles. The interactions between atoms separated by at least three bonds are described by a pairwise additive 1–6–12 potential. The parameters are taken from the AMBER force field.<sup>30</sup> In previous calculations on 222 in vacuo, we used the united atom representation for  $\text{CH}_2$  groups, but it is more appropriate

(16) Wipff, G.; Weiner, P.; Kollman, P. A. *J. Am. Chem. Soc.* **1982**, *104*, 3249–3258.

(17) Howard, A. E.; Singh, U. C.; Billeter, M.; Kollman, P. A. *J. Am. Chem. Soc.* **1988**, *110*, 6984–6991.

(18) van Eerden, J. V.; Harkema, S.; Feil, D. *J. Phys. Chem.* **1988**, *92*, 5076–5079.

(19) Straatsma, T. P.; McCammon, J. A. *J. Chem. Phys.* **1989**, *91*, 3631–3637.

(20) Dang, L. X.; Kollman, P. A. *J. Am. Chem. Soc.* **1990**, *112*, 5716–5720.

(21) Mazor, M. H.; McCammon, J. A.; Lybrand, T. P. *J. Am. Chem. Soc.* **1990**, *112*, 4411–4419.

(22) Wipff, G.; Kollman, P. A. *New J. Chem.* **1985**, *9*, 457–465.

(23) Geue, R.; Jacobson, S. H.; Pizer, R. *J. Am. Chem. Soc.* **1986**, *108*, 1150–1155.

(24) Wipff, G.; Wurtz, J. M. In *Dynamics Views of Macrocyclic Receptors: Molecular Dynamics Simulations and Normal Modes Analysis*; Pullman, R., Ed.; Reidel: Dordrecht, 1988; p 1.

(25) Auffinger, P.; Wipff, G. *J. Comput. Chem.* **1990**, *11*, 19–31.

(26) Howard, A. E.; Kollman, P. A. *J. Med. Chem.* **1988**, *32*, 1669–1675.

(27) Saunders, M.; Houk, K. N.; Wu, Y. D.; Still, W. C.; Lipton, M.; Chang, G.; Guida, W. C. *J. Am. Chem. Soc.* **1990**, *112*, 1419–1427.

(28) Heeg, M. J. *Acta Crystallogr.* **1988**, *C44*, 2219–2220.

(29) Singh, C.; Weiner, P. K.; Caldwell, J.; Kollman, P. A. *Amber 3.0*, University of California, San Francisco, 1987.

(30) Weiner, S. J.; Kollman, P. A.; Nguyen, D. T.; Case, D. A. *J. Comput. Chem.* **1986**, *7*, 230–252.

to represent explicitly these hydrogens in water to better describe the solvation pattern. The atomic charges have been fitted on electrostatic potentials calculated *ab initio* at the 6-31G\* level on representative fragments.<sup>31</sup> They are reported in Figure 3.

Note that the oxygen atoms have larger charges ( $q_{\text{O}} = -0.405$ ) than in our previous studies fitted on the dipole moments of  $\text{OMe}_2$ .<sup>22</sup> These increased charges may partly compensate for the lack of a polarization term in the force field and for polarization effects of surrounding water molecules. The 1–4 electrostatic and van der Waals interactions have been calculated without scaling factor, since no definitive conclusion could be drawn concerning which factor should be most appropriate for similar calculations involving the OCCO fragment.<sup>32</sup> For water, the TIP3P potentials<sup>33</sup> were used.

For the calculations on cation complexes, the van der Waals parameters for  $\text{Na}^+$ ,  $\text{K}^+$ ,  $\text{Rb}^+$ , and  $\text{Cs}^+$  are the same as in ref 22. Those of  $\text{Li}^+$  come from ref 34. The  $\text{M}^{2+}$  and  $\text{M}^{3+}$  cations were modeled with the same  $\epsilon$  and  $\text{R}^*$  parameters as  $\text{Na}^+$  but with charges of +2 and +3, respectively. This corresponds approximately to the  $\text{Ca}^{2+}$  and  $\text{Eu}^{3+}$  cations, whose ionic radii in water (respectively, 1.03 and 1.06 Å) are comparable to that of  $\text{Na}^+$  (0.97 Å).<sup>35</sup> The charges of 222 in the cryptates were kept the same as for the cryptand, thus not taking into account the polarization induced by the cations. This approximation is consistent with keeping constant charges for the solvent, as done in most of the calculations performed on cation hydration,<sup>35–38</sup> and emphasizes electrostatic effects of the cation on hydration of the cryptates compared to the cryptand.

For the simulations on the 222 cryptates, we started from the **K** conformation of the cryptand with the cation at the center of the cage as found in the solid state.<sup>1</sup> The  $\text{Na}^+$ ,  $\text{K}^+$ ,  $\text{Rb}^+$ , and  $\text{Cs}^+$  cryptates can adopt similar conformations in the solid state with three gauche OC–CO dihedral angles. Their bridges are  $\text{g}^+\text{ttg}^+\text{ttg}^+$ , different from the  $\text{Ca}^{2+}$  cryptates in the solid state, which are  $\text{g}^-\text{tg}^-\text{g}^-\text{tg}^-$ .<sup>1</sup> The X-ray structures reported for  $\text{M}^{3+}$  are unsymmetrical due to the coordination of the cations to  $\text{NO}_3^-$  or  $\text{ClO}_4^-$  anions,<sup>39–42</sup> and significant distortions are observed.  $\text{Li}^+$  is weakly complexed by 222 in water ( $\log K_s = 1.25^4$ ), and no X-ray structure has been reported. The most closely related one corresponds to the  $\text{Li}^+$  inclusive complex of a benzo derivative of 222,<sup>43</sup> which has OC–CO and NC–CO gauche angles. The conformation of 222 in these  $\text{Li}^+$ ,  $\text{Ca}^{2+}$ , and  $\text{Eu}^{3+}$  cryptates may not be the same as in the  $\text{K}^+$  cryptates, but starting from the same **K** conformer remains reasonable and allows for more consistent comparisons along the series.

Each conformer has been placed at the center of a cubic water box of  $30 \times 30 \times 30$  Å. Removal of the solvent molecules at contact left respectively 816, 813, 816, and 819 water molecules for the **II**, **OO**, **SS**, and **K** forms, for uncomplexed 222. After 100 steps of molecular mechanics optimization, the systems were equilibrated for 6 ps of MD at 300 K and 1 atm starting with random velocities. This was followed by 45 ps of MD. Periodic boundary conditions were used with a residue-based cut-off of 8.0 Å for nonbonded interactions. The Verlet algorithm was used with a time step of 2 fs. The C–H bonds of 222 and the O–H and H···H distances of  $\text{H}_2\text{O}$  were constrained to constant values by SHAKE.<sup>44</sup> Coordinates were saved every 0.01 ps. Each simulation took about 20 h of CPU time on an IBM-3090-600 VF. For the simulations in vacuo, performed for comparison, a similar procedure was used for consistency.

The MDNM graphics software was used to visualize the hydration pattern of 222.<sup>45</sup> Plots of radial distribution functions and calculation

**Table I.** 222 Cryptand: Energy Component Analysis (kcal/mol)

conformation	II	OO	SS	K
$\langle E_{\text{sw}} \rangle^{a,b}$	-49 (5)	-48 (5)	-42 (4)	-79 (5)
$\langle E_{222} \rangle$	27 (4)	29 (4)	25 (4)	39 (4)
$\Delta E_{\text{opt}}^c$	0	1	-1	9
$\langle E_{\text{sw}} \rangle^d$	-7924 (83)	-7886 (82)	-8020 (79)	-7939 (81)
$\langle E_{\text{sw}} \rangle^d$	-7953	-7944	-8049	-7939
$\langle E_{\text{total}} \rangle$	-7975	-7963	-8067	-7979
Contribution of the 6 Oxygens, 2 Nitrogens, and 18 $\text{CH}_2$ to $E_{\text{sw}}$				
O	-44 (19)	-48 (20)	-25 (17)	-89 (16)
N	-2 (2)	-5 (2)	-1 (2)	-9 (2)
$\text{CH}_2$	-3 (12)	5 (12)	-17 (12)	19 (12)

<sup>a</sup> Energies are calculated with a residue-based cut-off of 8 Å. <sup>b</sup> Values in parentheses correspond to calculated fluctuations. <sup>c</sup> Relative energies for 222 optimized in vacuo. <sup>d</sup> Corrected for 819 water molecules.

**Table II.** 222 Cryptand: Occurrence (%) of Solute/Solvent Hydrogen Bonds during the MD Simulations

conformation	II	OO	SS	K
$\text{O} \cdots \text{HOH}^a$	71.3	61.8	63.9	93.4
$\text{N} \cdots \text{HOH}^a$		15.8		
Total Number of Water Molecules Involved in Hydrogen Binding to 222 <sup>b</sup>				
	30	21	35	3

<sup>a</sup> The hydrogen bond criterion used is the following: The  $\text{X} \cdots \text{H}-\text{O}$  distance is smaller than 2.5 Å, and the angle  $\text{X} \cdots \text{H}-\text{O}$  is larger than  $135^\circ$ . <sup>b</sup> The hydrogen bonds occurring for less than 2% have been discarded.

of solute/solvent interaction energies were performed by using adapted analysis modules of GROMOS<sup>46</sup> that were interfaced to AMBER output.

In the following, we denote **II**, **OO**, **SS**, and **K** the *unique* conformations of 222 coming from the solid-state structures and which correspond to local energy minima.<sup>22,25</sup> During the MD simulations, conformational transitions may occur for **II**, **OO**, **SS**, and **K**, in vacuo and in solution, but we continue to refer to these *dynamic structures* by using a similar nomenclature, i.e., **II**, **OO**, **SS**, and **K**.

## Results

**1. Hydration of the 222 Cryptand.** In the following, we provide evidence for the particular hydration pattern of the **K** form, which displays significant stabilization, compared to the other conformers. This is supported by an energy component analysis and by structural analysis.

**a. Energy Analysis.** The average solute/solvent interaction energies  $E_{\text{sw}}$  calculated for each of the conformers (Table I) are in several respects unexpected and do not follow the qualitative predictions based on the solvent accessible surface of heteroatoms. There is no significant difference in the  $E_{\text{sw}}$  energies for **II**, **OO**, and **SS** (respectively, -49, -48, and -42 kcal/mol), whereas the cryptate type **K** conformer, which we anticipated to be the least well hydrated, has significantly better interactions with water ( $E_{\text{sw}} = -79$  kcal/mol)! This preference for the **K** form of about 30 kcal/mol is significantly larger than the calculated fluctuations on these numbers (about 5 kcal/mol).

This result deserves further analysis, and we first divide  $E_{\text{sw}}$  into contributions from the six oxygens, the two nitrogens, and the eighteen  $\text{CH}_2$  groups of the solute. Values reported in Table I are the average of these group contributions over all the saved configurations. For each conformer, the contribution of the 2 nitrogens is weak (-1 to -9 kcal/mol), the contribution of the 18  $\text{CH}_2$  may be negative (**II**, **SS**) or positive (**OO**, **K**), while the contribution of the 6 oxygens is the most negative (from -25 to -89 kcal/mol). It is also the largest for the **K** form despite the converging orientation of its oxygens. Conversely, it is weakest in the **SS** form, where oxygens are diverging and have the largest accessible surface to the solvent! There are differences in the other components of  $E_{\text{sw}}$  as well, some of which are easier to rationalize. For instance, the nitrogen contribution is more negative for the *out-out* form **OO** (-5 kcal/mol) than for *in-in* conformers **II** or **SS** (-2 and -1 kcal/mol). For **K**, however, this contribution is

- (31) Grootenhuis, P. Private communication, 1988.  
 (32) Billeter, M.; Howard, A. E.; Kuntz, I. D.; Kollman, P. A. *J. Am. Chem. Soc.* **1988**, *110*, 8385–8391.  
 (33) Jorgensen, W. L.; Chandrasekhar, J.; Madura, J. D. *J. Chem. Phys.* **1983**, *79*, 926–936.  
 (34) Kollman, P. A.; Wipff, G.; Singh, U. C. *J. Am. Chem. Soc.* **1985**, *107*, 2212–2219.  
 (35) Marcus, Y. *Chem. Rev.* **1988**, *88*, 1475–1498.  
 (36) Clementi, E.; Barsotti, R. *Chem. Phys. Lett.* **1978**, *59*, 21–25.  
 (37) Marchese, F. T.; Beveridge, D. L. *J. Am. Chem. Soc.* **1984**, *106*, 3713–3720.  
 (38) Heinzinger, K. *Pure Appl. Chem.* **1985**, *57*, 1031–1042.  
 (39) Hart, F. A.; Hursthouse, M. B.; Malik, K. M. A.; Moorhouse, S. J. *Chem. Soc., Chem. Commun.* **1978**, 549–550.  
 (40) Burns, J. H. *Inorg. Chem.* **1979**, *18*, 3044–3048.  
 (41) Ciampolini, M.; Dapporto, P.; Nardi, N. *J. Chem. Soc., Dalton Trans.* **1979**, 974–980.  
 (42) Bünzli, J. C. In *Complexes with Synthetic Inophores*; Gschneidner, K. A., Jr., Eyring, L., Eds.; Elsevier Science Publishers: London, 1987; pp 321–394.  
 (43) Ward, D. L.; Rhinebarger, R. R.; Popov, A. I. *Inorg. Chem.* **1986**, *25*, 2825–2827.  
 (44) Ryckaert, J. P.; Ciccolini, G.; Berendsen, H. J. C. *J. Comput. Phys.* **1977**, *23*, 327–336.

- (45) Wipff, G.; Wurtz, J. M. *MDNM: a program to display Molecular Dynamics or Normal Modes of vibrations on the PS300*, 1987.  
 (46) van Gunsteren, W. F.; Berendsen, H. J. C. *Groningen Molecular Simulation (GROMOS) Library Manual Biomos*, Groningen, 1987.

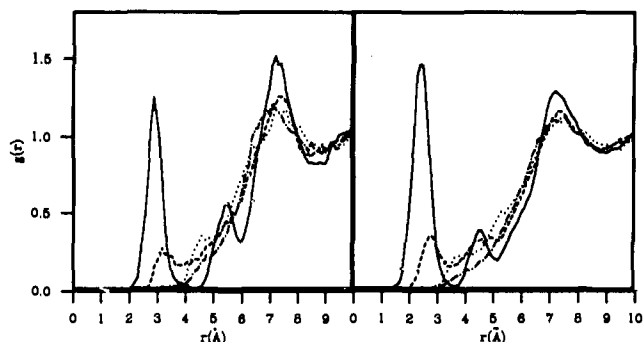


Figure 4. Radial distribution functions of water ( $O_w$  left and  $H_w$  right) around the center of mass of 222 uncomplexed (conformations II, ---; OO, - - -; SS, ····; K, —).

still more negative ( $-9$  kcal/mol), which suggests that the core of **K** may be accessible to water. Clearly, more detailed knowledge of water structure around the solute is required, and we analyzed therefore the hydrogen bond pattern and the radial distribution functions and displayed graphical representation of selected solute/water "supermolecules".

**b. Hydrogen Bond Analysis from Radial Distribution Functions and Graphical Display. Why and How Is the K Conformer so Well Hydrated?** A detailed hydrogen bond analysis involving the N and O atoms of the solute and  $H_w$  atoms of water at less than 2.5 Å and in a "linear" arrangement (see Table II) has been performed. The results confirm that the *in-in* forms II, SS, and K are hydrogen bonded to water via their oxygens only, whereas for the OO form, hydrogen bonding involves also the nitrogen atoms. The K form displays the interesting feature that its oxygens are most of the time (93.4%) hydrogen bonded with only three water molecules. For the other forms, there are more than 20 water molecules hydrogen bonded for about 60% of the simulation.

The radial distribution functions (rdf's) of water around the center of mass (Figure 4) of the solute have been calculated. The curves cannot be interpreted simply as for spherical substrates. They display however a specific pattern for the K form, compared to II, OO, and SS.

The center of mass...water rdf's show first that *none of the structures has water inside the cage*: The smallest center of mass... $O_w$  distances found along the simulations are 1.9, 2.5, 3.0, and 3.4 Å for the K, OO, SS, and II forms, respectively. This is expected for II, OO, and SS structures that lack an adequate cavity to form inclusion complexes. For the K form, however, no water takes the place of the potential host cation. There are instead three water molecules close to the core, as evidenced by the first peak at 2.3 Å in the center of mass... $H_w$  and at 3.0 Å in the center of mass... $O_w$  curves. Integration of those peaks leads respectively to 5.9 for  $H_w$  and 3.0 for  $O_w$ , i.e., to three water molecules. Firm bonding of those molecules to the K form during the 45 ps is shown by the fact that the rdf's drop to zero after these first peaks. For the other forms, no clear pattern is found, except for OO, where two peaks (respectively, at 3.0 and 3.2 Å) correspond to one water molecule bound to 222. For the K form only, there is in addition a clear second peak, at 5.3 Å in the center of mass... $O_w$  rdf, corresponding to six water molecules. It is followed by a third peak at about 7.5 Å, which appears also for the other conformers.

Dynamic representations on the graphics system and a stereo view (Figure 5) show a typical hydration pattern of K. There are three water molecules closest to the center of mass, making an arrangement of approximate  $D_3$  symmetry. Each of them sits between two bridges of the cryptand and makes two  $H_w\cdots O$  hydrogen bonds (of about 1.8 Å) with ether oxygens of the adjacent chains.

In the K form, each water proton  $H_w$  is at about 2.8 Å from the nitrogen bridgeheads. This observation may explain why the hydration energy of the N bridgeheads is larger in K than in OO (Table I). There is no diffusion of these three water molecules during the 45 ps of MD due to their strong attraction with 222.

A concerted exchange mechanism involving other water molecules would be difficult because of steric congestion. Each of these facial water molecules is also hydrogen bonded to two interbridging "second-shell" water molecules (Figure 5), which contributes to their low mobility in water and accounts for the second peak at 5.3 Å in the center of mass... $O_w$  rdf of K (Figure 4).

We checked that the preference for three bridging water molecules over water complexed *inside* the cage is not an artifact attributable to the starting configuration, by running another MD simulation starting with a water molecule set at the center of the cavity. This was achieved by taking the structure of the  $NH_4^+$  cryptate<sup>47</sup> with two instead of four NH protons. During the first ps of simulation, this water moved to one face and two water molecules became doubly hydrogen bonded to adjacent chains of 222. After two additional ps, the hydration pattern was similar to that discussed above.

The angular distribution of water in the first hydration shell of the  $CH_2$ , N, and O groups calculated within respectively 4.3, 4.3, and 3.4 Å of the solute (first minima of the rdf's) further reveals the hydration pattern and the specificity of the K form. Figure 6 shows schematic orientations of water around a methyl group and around an oxygen atom (see ref 48). Typical values of  $\theta$  are about  $0^\circ$  and  $90^\circ$  in the first case and  $60^\circ$  and  $180^\circ$  in the second. The distributions of  $\cos \theta$  (Figure 6) are consistent with the hydrophobic character of  $CH_2$  groups, more pronounced for K than for the other forms. Indeed, angular distributions are maximum around 0 and +1. The unique peak at about 0.6 for K corresponds to the three interbridged water molecules. Around the nitrogen bridgeheads, there are no clear orientational preferences for II, OO, and SS, in contrast to K with peaks at  $-0.5$  and 0.2. Around the oxygens, there is a marked orientational preference (peaks at about  $-1.0$  and 0.6), especially for the K form.

**c. Interaction Energies of Water Molecules Hydrogen Bonded to the Cryptand. From Quasi-Complexed to Very Labile Water Depending on the Conformation of the Solute.** We followed along the MD simulations the interaction energy between 222 and some of the most frequently hydrogen bonded water molecules. For those molecules *i*, their interaction energy  $E_{s-i}$  with 222 was recalculated along the simulation. In Figure 7 are plotted such typical  $E_{s-i}$  that are related to different modes of binding to the solute, as a function of its conformation. For the K form, the three bonded water molecules display a similar behavior and  $E_{s-i}$  fluctuate around  $-13$  kcal/mol, consistent with the quasi permanent bridging position of these three water molecules (see for instance  $E_{s-497}$ ), and close to the optimal interaction energy. Molecular mechanics optimizations on this  $222/(H_2O)_3$  supermolecule using the same empirical energy parameters give an interaction energy of about 13 kcal/mol between each water molecule and 222. They form with the solute a fairly stable complex or supermolecule related to their bridging position. For the OO form, water molecules 708 and 311 are the most often hydrogen bonded to 222. Plots of  $E_{s-708}$  and  $E_{s-311}$  demonstrate that they may have strong interactions with 222 (about  $-10$  kcal/mol) and that, at about 30 ps, they exchange one with the other. Interestingly, the moiety of 222 bound to these water molecules has a conformation similar to that of the K form. It is also reminiscent of 18-crown-6 in its  $D_{3d}$  symmetry. For SS, the situation is still different. Despite the *out* orientation of the oxygen binding sites, the most frequently coordinated water molecules (371 for example) are weakly bound (by about  $-3$  kcal/mol or less), and for shorter times (about 10–20 ps), and have therefore largest mobility. They make linear, rather than bridged, hydrogen bonds.

From these selected examples, it appears that the structure and mobility of water molecules hydrogen bonded to the solute depend markedly on the conformation of the latter and on topological features. As found for 18-crown-6,<sup>49</sup> bridging hydration is

(47) Dietrich, B.; Kintzinger, J. P.; Lehn, J. M.; Metz, B.; Zahidi, A. J. *Phys. Chem.* **1987**, *91*, 6600–6606.

(48) Remerie, K.; van Gunsteren, W. F.; Engberts, J. B. F. N. *Mol. Phys.* **1985**, *56*, 1393–1409.

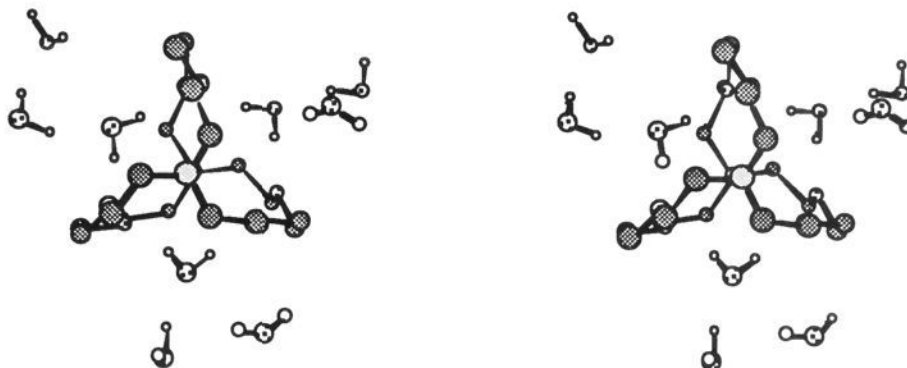


Figure 5. 222 cryptand: stereoview of the hydrated K form. We represent only the first and second water shell around its center of mass.

Table III.  $M^{n+}/222$  Cryptates: Analysis of Average Hydration Energies<sup>a,b</sup>

cation	$E_{s/w}^c$	$E_{222/w}^d$	$E_{M^{n+}/w}^e$	$E_{ww}^f$	groups of 222 <sup>g</sup>		
					6 (O)	18 (CH <sub>2</sub> )	2 (N)
none		-79 (5)		-7939 (81)	-89 (15)	19 (12)	-9 (2)
Li <sup>+</sup>	-151 (7)	-16 (6)	-138 (8)	-7910 (83)	143 (17)	-178 (12)	19 (2)
Na <sup>+</sup>	-90 (7)	-12 (5)	-78 (9)	-7923 (79)	149 (16)	-180 (12)	20 (2)
K <sup>+</sup>	-87 (7)	-13 (5)	-74 (10)	-7912 (81)	147 (17)	-180 (13)	20 (2)
Rb <sup>+</sup>	-86 (7)	-15 (6)	-70 (9)	-7918 (82)	143 (17)	-177 (12)	19 (2)
Cs <sup>+</sup>	-84 (7)	-17 (5)	-68 (8)	-7922 (80)	137 (16)	-173 (13)	19 (2)
Ca <sup>2+</sup>	-366 (12)	36 (6)	-401 (14)	-7759 (80)	340 (19)	-348 (13)	44 (2)
Eu <sup>3+</sup>	-812 (23)	80 (7)	-891 (24)	-7520 (84)	505 (17)	-491 (14)	65 (2)

<sup>a</sup> Energies (kcal/mol) calculated with a cut-off of 8 Å for interactions involving water. <sup>b</sup> Value in parentheses correspond to calculated fluctuations. <sup>c</sup> Average interaction energy between the  $M^{n+}/222$  cryptate and water. <sup>d</sup> Average interaction energy between the cage and water. <sup>e</sup> Average interaction energy between the  $M^{n+}$  cation and water. <sup>f</sup> Average water-water interaction energy. <sup>g</sup> Average interaction energy between each group of atoms of 222 and water.

strongest and displays weakest mobility compared to hydration through linear hydrogen bonds.

**2. Hydration of the  $M^{n+}/222$  Cryptates.** In this section, based on energy and structural analysis, we provide evidence for cation-dependent direct and long-range interactions between water and the encapsulated cations. The simulations allow also for a comparison of the coordination number of the various cations uncomplexed or complexed by 222 in water.

**a. Energy Results.** The hydration energy  $E_{sw}$  corresponding to the water molecules within 8 Å of the cryptates are reported in Table III as well as various components of  $E_{sw}$  based on the contributions of the cation and the cage and on the N, O, and CH<sub>2</sub> groups of 222. These results show that even monocharged cations induce a significant reorganization of water around 222 cryptate, as compared to the cryptand. For the Na<sup>+</sup>, K<sup>+</sup>, Rb<sup>+</sup>, and Cs<sup>+</sup> cryptates, the total  $E_{sw}$  (from -90 to -84 kcal/mol) is comparable to that found above for 222 uncomplexed (-79 kcal/mol for K). The largest contributions come, however, from the cation (from -78 to -68 kcal/mol) rather than from the cage itself (-12 to -17 kcal/mol), which is poorly hydrated compared to the free state. The Li<sup>+</sup> cryptate clearly does not fit in the series and has the most negative  $E_{sw}$ . This is because Li<sup>+</sup> is too small for the cavity of 222 and moved from a central to a facial position during the dynamics to achieve a better hydration (see next and Figure 10).

As expected, interactions of the cryptates with water increase with their charges. The Ca<sup>2+</sup> and Eu<sup>3+</sup> cryptates have very negative  $E_{sw}$  energies (-366 and -812 kcal/mol), dominated by the cation contributions, whereas water interactions with 222 become repulsive (+36 and +80 kcal/mol). The increased electric field induces significant water structure around the cryptate (like in the bulk water), and the screening effect of the cage is not very effective. Consistently, the water-water interaction energies  $E_{ww}$  decrease from -7923 for Na<sup>+</sup> to -7520 kcal/mol for Eu<sup>3+</sup> (Table III). For Na<sup>+</sup> and K<sup>+</sup> cryptates,  $E_{ww}$  is comparable to the value obtained for the uncomplexed K form.

Table IV.  $M^{n+}/222$  Cryptates: Average Energy Components

	$\langle E_{int} \rangle^a$	$\langle E_{222} \rangle$	$\langle E_{tot} \rangle^b$	$E_{opt}^c$
none		39 (4)		
Li <sup>+</sup>	-77 (4)	38 (4)	-39 (5)	-82
Na <sup>+</sup>	-85 (3)	41 (5)	-44 (5)	-79
K <sup>+</sup>	-74 (2)	36 (3)	-38 (4)	-70
Rb <sup>+</sup>	-63 (2)	34 (3)	-29 (4)	-61
Cs <sup>+</sup>	-48 (2)	35 (4)	-13 (4)	-45
Ca <sup>2+</sup>	-173 (4)	42 (4)	-131 (5)	-181
Eu <sup>3+</sup>	-259 (8)	48 (5)	-211 (7)	-289

<sup>a</sup> Average interaction energy between the cation and 222. The fluctuations are in parentheses. <sup>b</sup> Average energy of the cryptate. <sup>c</sup> Energy of the cryptates optimized by MM in vacuo.

Contributions of the two N, six O, and eighteen CH<sub>2</sub> to the "hydration energy"  $E_{sw}$  of the cryptate reveal opposite trends compared to the cryptand. In the cryptates (Table III), both O and N contributions to  $E_{sw}$  are positive instead of being negative, whereas the CH<sub>2</sub> contributions become attractive. These energy components increase markedly with the charge of the solute (in the Na<sup>+</sup>, Ca<sup>2+</sup>, Eu<sup>3+</sup> series) but are not very sensitive to the size of monocharged substrates (in the Li<sup>+</sup> to Cs<sup>+</sup> series).

It is interesting to compare these  $E_{sw}$  hydration energies of the cryptate, to the corresponding interaction energies  $E_{int}$  between the cation and the cage within the complexes (Table IV). For K<sup>+</sup> and Na<sup>+</sup>, the latter (-85 and -74 kcal/mol) are in the same order of magnitude as  $E_{sw}$ , whereas for Ca<sup>2+</sup> and Eu<sup>3+</sup> cryptates  $E_{int}$  (-192 and -259 kcal/mol) is significantly smaller than  $E_{sw}$  (-324 and -812 kcal/mol), which indicates that first-shell coordination provides the most important stabilization. For the highly charged Ca<sup>2+</sup> and Eu<sup>3+</sup> cryptates, second- and third-shell effects become more important. As found from gas-phase optimizations,<sup>22</sup>  $E_{int}$  decreases from Na<sup>+</sup> to Cs<sup>+</sup>. For Li<sup>+</sup> and Cs<sup>+</sup>,  $E_{int}$  is weaker than for K<sup>+</sup>, the best recognized alkali cation, but for different reasons. Intrinsically, Li<sup>+</sup> has larger interactions with oxygen binding sites than K<sup>+</sup>,<sup>50</sup> but the cation is too small for 222 and requires additional coordination by water. This

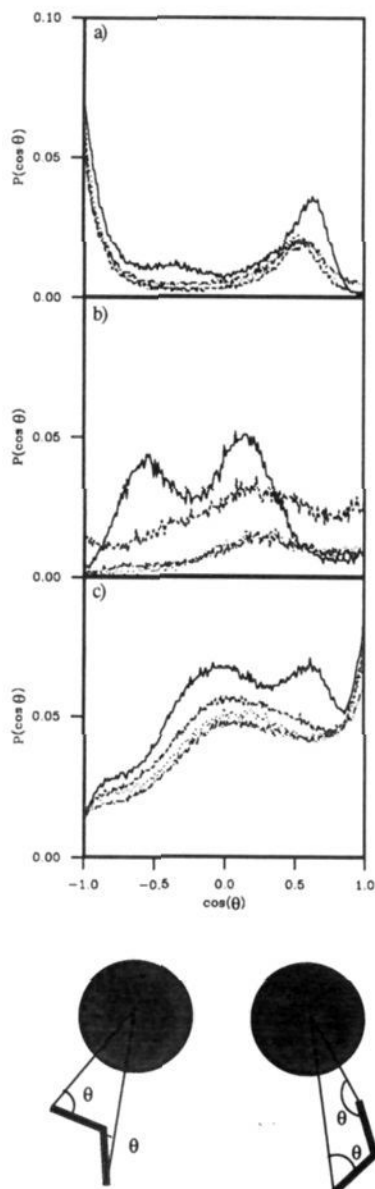


**Figure 6.** 222 cryptand: distributions of orientation of water molecules in the first hydration shells of groups of 222 (a) O...H<sub>2</sub>O, (b) N...H<sub>2</sub>O, and (c) CH<sub>2</sub>...H<sub>2</sub>O (conformations II, ...; OO, ---; SS, -.-; K, —). The angle  $\theta$  between one center and the H-O bond (X...H-O) is shown for typical orientations of water around a methyl group (left) and an oxygen (right).

contrasts with Cs<sup>+</sup>, which is somewhat too big and has weaker interactions with 222 and with water but sits at the center of the cage.

Finally, dynamic effects and interactions with water lead to a significant destabilization of the cryptates compared to the gas-phase energy minima. Their average total energies in water are higher than the energies optimized in vacuo (Table IV).

**b. Hydration Pattern of the Cryptates.** These are revealed by the rdf's around the cations, the center of mass of the cryptates (Figures 8 and 9), the O, N, and CH<sub>2</sub> groups,<sup>51</sup> and a detailed analysis of the solvent molecules coordinated to the cation (Table V). See also snapshots in Figure 10. If the cations were at the center of the cavity, the center of mass...water rdf's would be identical with the M<sup>n+</sup>...water rdf's (Figures 8 and 9). In fact, they are not because most cations move more or less to the solvent, depending on their size and charge. This is characterized also by the average (center of mass...M<sup>n+</sup>) distances (Table VI). In

**Table V.** M<sup>n+</sup>/222 Cryptates: List of the Water Molecules Coordinated to the Cation

M <sup>n+</sup>	n <sup>o</sup> H <sub>2</sub> O	(d <sub>M<sup>n+</sup>...O<sub>w</sub></sub> )	occurrence (%)	first peak	first min	CN <sup>a</sup>
Li <sup>+</sup>	372	1.8	100	1.8	2.5	2.0
	412	1.8	100			
Na <sup>+</sup>	349	2.6	90	2.6	3.5	0.9
	370	3.1	80	3.0	4.2	1.4
Rb <sup>+</sup>	535	3.1	19			
	340	3.4	19	3.2	4.4	1.3
Cs <sup>+</sup>	387	3.4	16			
	410	3.2	18			
	756	3.4	43			
	361	3.7	65	3.4	4.4	1.3
Ca <sup>2+</sup>	372	3.7	16			
	492	3.7	24			
	372	2.3	100	2.4	2.8	3.0
Eu <sup>3+</sup>	396	2.3	100			
	438	2.3	100			
	362	2.3	94	2.3	2.8	3.9
	372	2.3	100			
	396	2.3	100			
	438	2.3	100			

<sup>a</sup>Coordination number of the complexed cation.

water, the largest value (1.6 Å) is found for Li<sup>+</sup> which lies in a facial rather than in an inclusive position. The smallest value (0.2 Å) is found for Cs<sup>+</sup>, which sits at the center of the cavity.

Comparison of the M<sup>n+</sup>...water rdf's in the cryptates with the center of mass...water rdf in the cryptand (K form) confirms the *change in hydration pattern induced by complexation*. Let us first consider the alkali cation cryptates. For cryptates of Na<sup>+</sup> to Cs<sup>+</sup>, there are water molecules directly coordinated to M<sup>n+</sup>, despite its inclusive position. These are characterized by a marked peak in the M<sup>n+</sup>...O<sub>w</sub> rdf's (from 2.6 to 3.4 Å) and in the M<sup>n+</sup>...H<sub>w</sub> rdf's (from 3.1 to 4.1 Å). The orientation of their dipole (Figures 4, 10 and 11a) is reversed, compared to that around the K form of the free ligand. Integration of the rdf's leads to coordination numbers (CN) of about 0.9 for Na<sup>+</sup> and ~1.3 for K<sup>+</sup>, Rb<sup>+</sup>, and Cs<sup>+</sup>. There is loss of C<sub>3</sub> symmetry for the solvent molecules close to the core for instant structures. The *dynamical coordination of water depends on the size of M<sup>n+</sup>*. Na<sup>+</sup> remains coordinated to a same water molecule for 90% of the time, whereas for K<sup>+</sup>, Rb<sup>+</sup>, and Cs<sup>+</sup>, there is an exchange between different water molecules (respectively, 2, 4, and 3; see Table V). The Li<sup>+</sup>/222 cryptate is of facial type, and two water molecules remain coordinated to Li<sup>+</sup> along the simulation (Figure 10). One H<sub>2</sub>O is held inside the cage by Li<sup>+</sup>, and the other is outside. This mode of binding of the Li<sup>+</sup>/H<sub>2</sub>O "inclusion complex" by 222 bears much resemblance with the X-ray structure of the complex formed by Li<sup>+</sup>/H<sub>2</sub>O and 18-crown-6<sup>52</sup> and with the water cryptate found for 222,1H<sup>+</sup>.<sup>53</sup> In all cases, the water protons are hydrogen bonded to ether oxygens of the opposed moiety to the Li<sup>+</sup> or N-H<sup>+</sup> binding sites (see Figure 9).

For Na<sup>+</sup>, Ca<sup>2+</sup>, and Eu<sup>3+</sup> cryptates, direct water coordination to the cation increases. Integration of the first peaks of the rdf's (Figure 9 and Table V) gives coordination numbers of 0.9 for Na<sup>+</sup>, 3.0 for Ca<sup>2+</sup>, and 3.9 for Eu<sup>3+</sup>. Although the cationic size is identical, the cation-water distance is somewhat smaller for Ca<sup>2+</sup> and Eu<sup>3+</sup> (about 2.3 Å) than for Na<sup>+</sup> (2.5 Å), as a result of stronger cation-water attractions. This may be also indicative of steric hindrance caused by 222 for optimal cation-water interactions. Increased water structure in that series is suggested by the fact that the first peaks in the rdf's become sharper from Na<sup>+</sup> to Eu<sup>3+</sup>. The residence time of these first-shell water molecules corresponds to about 100% of the simulation, with no exchange (Table V).

In the Na<sup>+</sup> to Cs<sup>+</sup> series, the second important peak in the M<sup>n+</sup>...water or center of mass...water rdf's is at about 7 Å only and comparable to that found around the uncomplexed K form.

(51) Auffinger, P. Thèse de Doctorat, Université Louis-Pasteur, Strasbourg, 1991.

(52) Groth, P. *Acta Chem. Scand.* **1982**, *A36*, 109-114.

(53) Auffinger, P.; Wipfl, G. *J. Inclusion Phenom.* **1991**, in press.

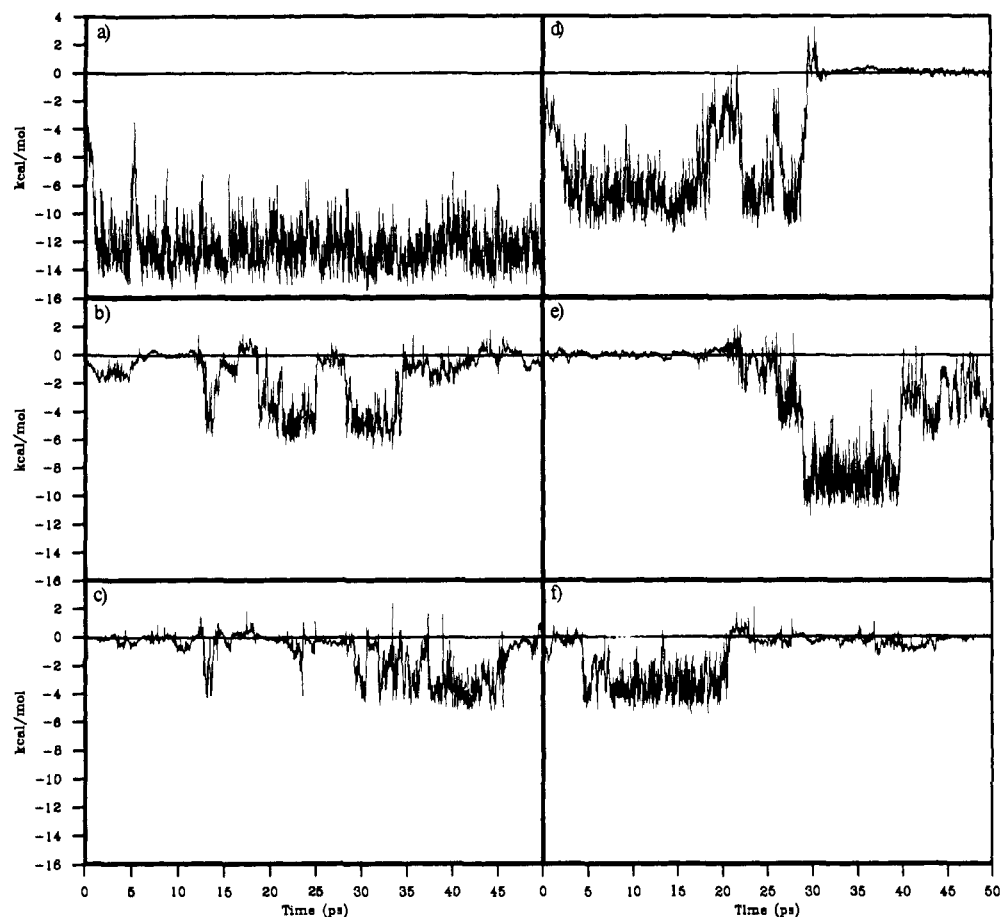


**Figure 7.** 222 cryptand: interaction energies of selected water molecules with 222 as a function of time (see text): (a) K form,  $E_{s-497}$ ; (b) II form,  $E_{s-351}$ ; (c) SS form,  $E_{s-371}$ ; (d) OO form,  $E_{s-331}$ ; (e) OO form,  $E_{s-708}$ ; (f) OO form,  $E_{s-333}$ .

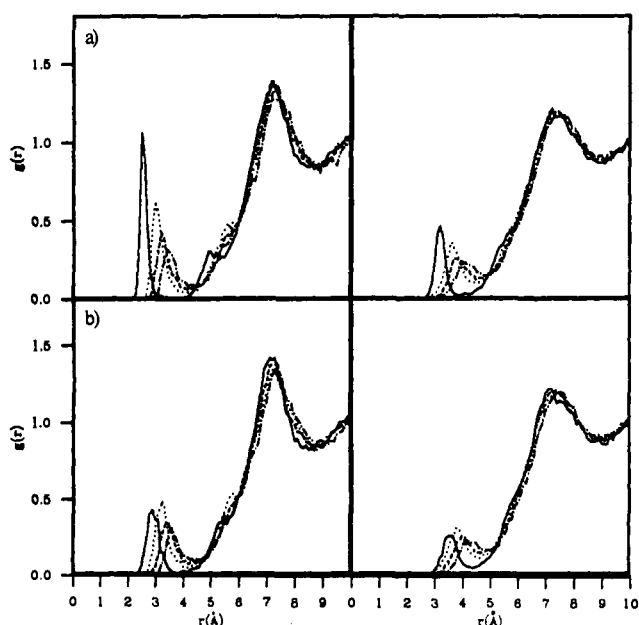


**Figure 8.**  $M^+/222$  cryptates: radial distribution functions of water ( $O_w$  left and  $H_w$  right) around (a) the cation ( $Na^+$ , —;  $K^+$ , ---;  $Rb^+$ , -.-;  $Cs^+$ , -.-) and (b) the center of mass of 222.

A similar peak was found by Pohorille et al. in their study of the highly charged  $SC_{24}H^+$  cryptand.<sup>54</sup> There is thus no significant water structure beyond the first hydration shell of the monovalent complexed cations. Figure 10 shows for the  $Na^+$  cryptate that

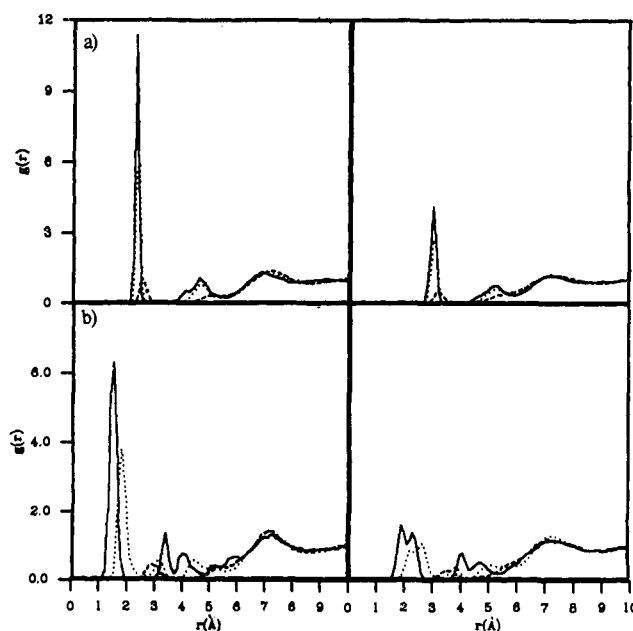


**Figure 9.**  $M^{2+}/222$  cryptates: radial distribution functions of water ( $O_w$  left and  $H_w$  right) around (a) the cation ( $Na^+$ , -.-;  $Ca^{2+}$ , ---;  $Eu^{3+}$ , —) and (b) the center of mass of 222.

the dipoles of water molecules not directly bound to  $Na^+$  can adopt different orientations and are not strongly influenced by  $Na^+$ .

For divalent or trivalent cation cryptates, water is structured in the second shell of the cation, i.e., between the bridges, and at larger distances, i.e., in the "hydrophobic"  $CH_2$  region. This is illustrated by Figure 10 and by the angular distribution of the water dipoles in the three first water shells around the  $Na^+$ ,  $Ca^{2+}$ ,

(54) Owenson, B.; MacElroy, R. D.; Pohorille, A. *THEOCHEM* 1988, 179, 467-484.

**Table VI.**  $M^{n+}/222$  Cryptates: Average Distance between the Center of Mass (CM) of the Cryptand and the Cation, Average N...N Distance, and Average Radius of Giration  $R_G^2$  of the Ligand<sup>a</sup>

	$(CM \cdots M^{n+})$		$(N \cdots N)$			$(R_G^2)^d$	
	vacuo	solution	vacuo	solution	opt	vacuo	solution
Li <sup>+</sup> <sup>b,c</sup>	0.6 (0.3)	1.6 (0.1)	5.9 (0.3)	6.2 (0.2)	5.5	13.7 (0.3)	16.4 (0.2)
Na <sup>+</sup>	0.3 (0.1)	0.5 (0.2)	6.2 (0.3)	6.1 (0.3)	5.8	15.7 (0.4)	16.0 (0.3)
K <sup>+</sup>	0.3 (0.1)	0.3 (0.1)	6.2 (0.2)	6.2 (0.2)	6.3	16.3 (0.3)	16.4 (0.2)
Rb <sup>+</sup>	0.4 (0.2)	0.3 (0.1)	6.3 (0.2)	6.3 (0.1)	6.3	16.5 (0.3)	16.6 (0.2)
Cs <sup>+</sup>	0.3 (0.1)	0.2 (0.1)	6.4 (0.1)	6.3 (0.1)	6.3	16.8 (0.3)	16.8 (0.2)
Ca <sup>2+</sup>	0.2 (0.1)	0.8 (0.2)	5.6 (0.2)	5.8 (0.2)	5.5	13.9 (0.3)	16.4 (0.2)
Eu <sup>3+</sup>	0.2 (0.1)	1.3 (0.1)	5.4 (0.2)	5.8 (0.1)	5.9	13.4 (0.3)	16.6 (0.2)

<sup>a</sup> Distances are in angstroms. The corresponding fluctuations are given in parentheses. <sup>b</sup> For the optimized structures, the cation is at the center of the cage for all cryptates, except for Li<sup>+</sup>/222 where Li<sup>+</sup> is in a facial position (at 1.8 Å from the center of 222). <sup>c</sup> During the MD simulation in water, Li<sup>+</sup> moved from the center of the cage to a facial position. <sup>d</sup>  $R_G^2$  is the square of the radius of giration of the 222 cryptand within the  $M^{n+}/222$  cryptates. See definition in the text.

**Table VII.** Hydration of  $M^{n+}$  Uncomplexed Cations: Analysis of the First Peak in the Cation-Water Radial Distribution Functions

$M^{n+}$	$M^{n+} \cdots O_w^a$ max (Å)	$M^{n+} \cdots H_w^b$ max (Å)	$M^{n+} \cdots O_w^c$ min (Å)	$M^{n+} \cdots H_w^d$ min (Å)	$n_{O_w}^e$	$n_{H_w}^f$
Li <sup>+</sup>	1.8	2.5	2.5	3.0	4.0	8.0
Na <sup>+</sup>	2.45	3.1	3.3	3.8	6.1	15.7
K <sup>+</sup>	2.9	3.6	3.6	4.5	7.7	24.4
Rb <sup>+</sup>	3.1	3.6	3.9	4.4	8.6	25.1
Cs <sup>+</sup>	3.3	3.7	4.3	5.1	<10.8	<34.4
Ca <sup>2+</sup>	2.35	3.1	3.1	3.7	7.9	15.9
Eu <sup>3+</sup>	2.3	2.95	2.9	3.8	8.9	17.6

<sup>a</sup> Maximum of the first peak in the  $M^{n+} \cdots O_w$  rdf. <sup>b</sup> Maximum of the first peak in the  $M^{n+} \cdots H_w$  rdf. <sup>c</sup> Minimum of the first peak in the  $M^{n+} \cdots O_w$  rdf. <sup>d</sup> Minimum of the first peak in the  $M^{n+} \cdots H_w$  rdf. <sup>e</sup> Coordination number for  $M^{n+} \cdots O_w$ . <sup>f</sup> Coordination number for  $M^{n+} \cdots H_w$ .

and Eu<sup>3+</sup> cryptates (Figure 11). The shells are defined by the rdfs of Figure 9 where  $\phi$  is the angle between  $M^{n+}$  and the water dipole. As expected, in the first shell, the water dipoles are reversed around the cryptates ( $\cos \phi$  peaks only at -1), in contrast to the K form uncomplexed where it peaks at +1.0. In the second shell, the unique peak at -1.0 broadens from Eu<sup>3+</sup> to Na<sup>+</sup>. In the third shell, water still orients preferentially with respect to Eu<sup>3+</sup> with a large peak at -1.0, but for Ca<sup>2+</sup> and Na<sup>+</sup> cryptates, its orientation is determined both by the cation and by the CH<sub>2</sub> groups. It differs therefore from that around the free ligand K.

**c. Comparison of the Coordination Number of  $M^{n+}$  Uncomplexed and in the  $M^{n+}/222$  Cryptates.** We performed a series of MD simulations on the alkali Ca<sup>2+</sup> and Eu<sup>3+</sup> cations in bulk water, to compare consistently their hydration in the free versus complexed state. Although, for the M<sup>+</sup> and M<sup>2+</sup> cations, numerous calculations based on Monte Carlo<sup>36,55</sup> or molecular dynamics<sup>38,56,57</sup> (see also ref 35 and references therein) have been reported, there are to our knowledge no such results concerning L<sup>3+</sup> cations, except a Monte Carlo simulation of Merbach et al.<sup>58</sup> and a molecular dynamics study of lanthanum chloride solutions.<sup>59</sup> Detailed results will be reported separately, and a summary of the analysis of the rdfs and energy results is given in Table VII. In the alkali cation series, integration of the first peaks of the  $M^{n+} \cdots O_w$  and  $M^{n+} \cdots H_w$  rdfs gives coordination numbers (CN) ranging respectively from 4.0 to 10.8 for O<sub>w</sub> and from 8.0 to 34.4 for H<sub>w</sub>, with distances ranging respectively from 1.8 to 3.3 Å and from 2.5 to 3.7 Å.

The CN of 7.9 calculated for Ca<sup>2+</sup> is smaller than the 9 or 10 values found by Palinkas et al. for typical D<sub>3h</sub> or D<sub>4d</sub> water structures<sup>60</sup> in 1.1 *m* CaCl<sub>2</sub> solution. For Eu<sup>3+</sup>, we find a CN of 9, to be compared with the 9.6 value determined from luminescence decay constants in water<sup>61</sup> and a value of 9.0 in solid-state structures.<sup>62</sup> This is also similar to the 9.0 value

**Table VIII.** 222 Cryptand: Average Atomic Fluctuations (Å) and Total Number of Dihedral Transitions (in Parentheses) Calculated in Vacuo and in Water

conformation	II	OO	SS	K
vacuo	0.85 (84)	0.65 (34)	0.82 (86)	0.72 (64)
aquo	0.35 (5)	0.46 (5)	0.33 (0)	0.31 (0)

**Table IX.** 222 Cryptand (K Form): Average Dihedral Angles in Water Compared to Molecular Mechanics (MM) Optimized Values

	from 45 ps of MD in water <sup>a</sup>	MM optimization in vacuo
NC-CO	-63.3 (9.3)	-71.3
OC-CO	54.0 (10.1)	82.8
CC-OC	-179.8 (10.5)	175.8
CC-NC <sup>b</sup>	163.1 (7.9)	154.6
CC-NC <sup>b</sup>	-69.0 (8.6)	-82.9

<sup>a</sup> The RMS fluctuations are given in parentheses. <sup>b</sup> They are six gauche and six trans CC-NC angles.

calculated by Monte Carlo<sup>58</sup> but is smaller than the 12.0 value calculated for La<sup>3+</sup> at infinite dilution.<sup>59</sup> The agreement is quite good given the neglect of three-body and polarization effects, which have been shown to influence markedly the CN of multivalent transition-metal cations in water.<sup>63</sup>

These numbers may be compared with the CN of the encapsulated ion, by assuming a contribution of 8 from the cage (two nitrogen and six oxygen binding sites) and adding the coordinated water molecules (Table V). For M<sup>+</sup> cryptates, from Li<sup>+</sup> to Cs<sup>+</sup>, the cation coordination is higher than or similar to that found in water. The same is found for Ca<sup>2+</sup> and Eu<sup>3+</sup> cryptates. The only exception is Cs<sup>+</sup>, which achieves slightly higher coordination in the uncomplexed state compared to the complex but forms weaker complexes than Na<sup>+</sup>, K<sup>+</sup>, or Rb<sup>+</sup>.<sup>14</sup> Although one of the leading concepts for designing macrocyclic receptors is to replace as much as possible the first solvation sphere of the ion by the binding sites of the receptor,<sup>64</sup> we find no simple correlation between the complex stability and coordination numbers. This is partly because longer range interactions with the solvent may play a significant role, especially for hard cations. Interestingly, however, in the M<sup>+</sup> series, the closest fit between CN for free and complexed cations corresponds to K<sup>+</sup> and Rb<sup>+</sup>, which have the most favorable enthalpy of complexation  $\Delta H_c$ .<sup>65,66</sup> For the Ca<sup>2+</sup> and Eu<sup>3+</sup> cryptates, the cation has a larger CN than in its free state. However, their  $\Delta H_c$  is zero or positive, due to prevention of second-sphere hydration, and in contrast to the alkali cation cryptates, these cryptates are of entropic rather than of enthalpic origin.<sup>65,66</sup>

(55) Mezei, M.; Beveridge, D. L. *J. Chem. Phys.* **1981**, *74*, 6902-6910.

(56) Bounds, D. G. *Mol. Phys.* **1985**, *54*, 1335-1355.

(57) Impey, R. W.; Madden, P. A.; McDonald, I. R. *J. Phys. Chem.* **1983**, *87*, 5071-5083.

(58) Helm, L.; Merbach, A.; Galera, S. Private communication, 1990.

(59) Meier, W.; Bopp, P.; Probst, M. M.; Spohr, E.; Lin, J. I. *J. Phys. Chem.* **1990**, *94*, 4672.

(60) Palinkas, G.; Heinzinger, K. *Chem. Phys. Lett.* **1986**, *126*, 251-254.

(61) Horrocks, W. D. J.; Sudnik, D. R. *J. Am. Chem. Soc.* **1979**, *101*, 334-340.

(62) Cossy, C.; Merbach, A. E. *Pure Appl. Chem.* **1988**, *60*, 1785-1796.

(63) Curtiss, L. A.; Halley, J. W.; Hautman, J.; Rahman, A. *J. Chem. Phys.* **1987**, *86*, 2319-2327.

(64) Lehn, J. M. *Struct. Bonding* **1973**, *161*, 1-69.

(65) Kauffmann, E.; Lehn, J. M.; Sauvage, J. P. *Helv. Chim. Acta* **1976**, *59*, 1099-1111.

(66) Yee, E. L.; Gansow, O. A.; Weaver, M. J. *J. Am. Chem. Soc.* **1980**, *102*, 2278-2285.

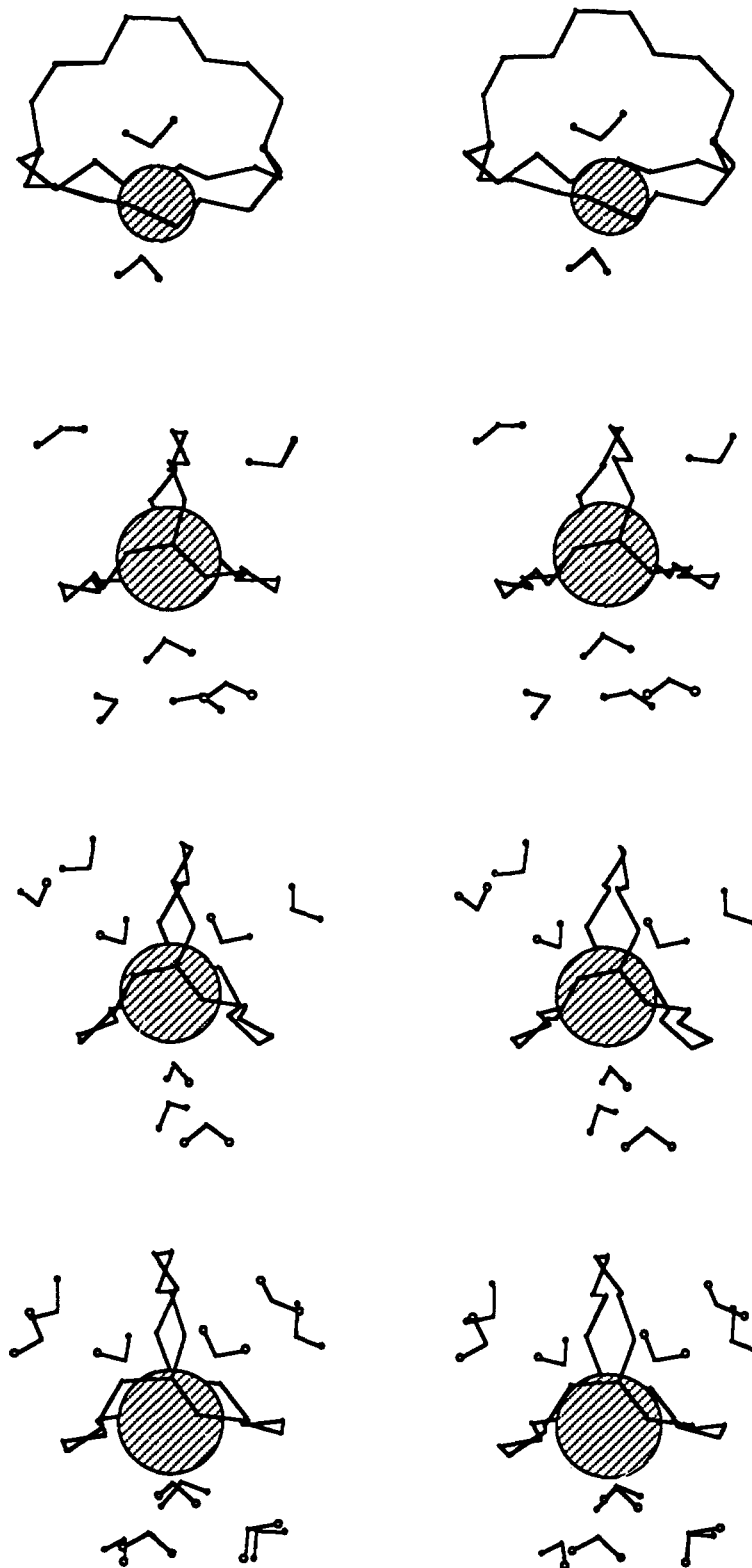


**Figure 10.** Stereoview of the hydrated  $\text{Li}^+$ ,  $\text{Na}^+$ ,  $\text{Ca}^{2+}$ , and  $\text{Eu}^{3+}$  cryptates. The water molecules in the first and second hydration shell of the cations are represented. For the  $\text{Li}^+$  cryptate, only the first shell of water molecules is represented.

**3. Gas-Phase versus Solution Structure and Dynamics of the Cryptand and of the Cryptates.** Detailed shapes and conformations of the cryptand and cryptates can be perturbed by solvation effects. Let us first consider the cryptand. During the simulations in vacuo, the **II**, **OO**, **SS**, and **K** structures are not conformationally stable within the 45 ps with the present force field (Table VIII). Each of them undergoes numerous dihedral transitions and fluctuates around one hypothetical average form with large RMS fluctuations (about 0.8 Å). Thus, *water reduces significantly the mobility of the cryptand*: In solution, the fluctuations are reduced by a

factor larger than 2 compared to the gas phase and the number of dihedral transitions drops down (Table VIII). The **SS** and **K** forms retain their conformation in solution; for **II** and **OO**, the overall shape and conformation remain close to the starting ones.

The *precise structure* of the cryptand differs also from gas phase to solution. Because of its  $D_3$  symmetry, the **K** form can be more easily analyzed, and we find that the gauche OC-CO and NC-CO dihedral angles are smaller in water ( $54 \pm 10^\circ$  and  $-63 \pm 10^\circ$ ) than in the optimized structure ( $83^\circ$  and  $-71^\circ$ ) (Table IX). This can be related to the three interbridging water molecules that

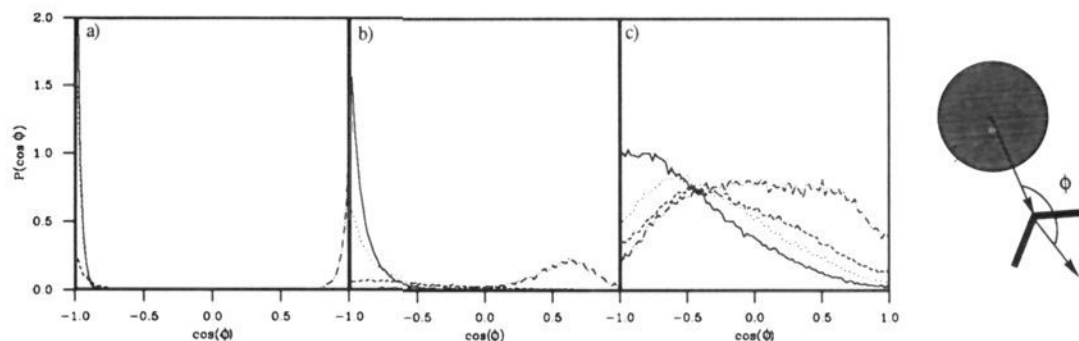


**Figure 11.** Distribution of  $\cos \phi$  for the water dipoles around the  $M^{**}$  cations of the cryptates or around the center of mass of the K form of the free cryptand.  $\phi$  is the angle between  $M^{**}$  (for the cryptates) or the center of mass (for the cryptand) and the bisector of HOH. (a), (b), and (c) correspond respectively to the first, second, and third water shells as defined by the rdf's ( $Na^+$ , ---;  $Ca^{2+}$ , ---;  $Eu^{3+}$ , —;  $K^+$ , -.-).

**Table X.** 222 Cryptand: Comparison of the N...N Distances (Å) for the Optimized Forms and from the MD Simulations, in Vacuo and in Water

conformation	II	OO	SS	K
vacuo <sup>a</sup>	5.5 (0.4)	6.2 (0.2)	5.2 (0.4)	6.1 (0.3)
aquo <sup>a</sup>	6.9 (0.1)	6.6 (0.2)	5.0 (0.2)	5.9 (0.2)
opt	6.9	6.7	4.9	6.5

<sup>a</sup>The RMS fluctuations are given in parentheses.

**Table XI.**  $M^{**}/222$  Cryptates: Average Fluctuations (Å) in Vacuo and in Water for the Cation and for the Cryptate

	vacuo <sup>a</sup>		solution	
	$M^{**}$	$M^{**}/222$	$M^{**}$	$M^{**}/222$
$Li^+$	0.38	0.58 (35)	0.67	0.32
$Na^+$	0.19	0.69 (30)	0.22	0.44
$K^+$	0.20	0.53 (11)	0.17	0.32
$Rb^+$	0.23	0.58 (10)	0.15	0.32
$Cs^+$	0.16	0.37 (0)	0.13	0.27
$Ca^{2+}$	0.10	0.63 (23)	0.20	0.24
$Eu^{3+}$	0.06	0.25 (5)	0.09	0.22

<sup>a</sup>The number of dihedral transitions is given in parentheses. In solution, no such transitions take place.

induce some strain in the cryptand.

The size of the cryptand, as characterized by the nitrogen...nitrogen distances  $d_{N...N}$  (Table X), differs from the gas phase to solution, but no simple trend is found. The II and OO structures are more elongated in solution than in vacuo, whereas for SS and K, the trend is reversed.

More regular trends can be found in the  $M^{**}/222$  cryptates. They are first of all rigidified compared to the cryptand due to the electrostatic and steric strain induced by the cation. This is observed in the gas phase by comparing for instance the K form uncomplexed with its cryptates (Tables VIII and XI). In solution, there is an additional decrease of mobility, of about 0.2 Å for 222/ $K^+$ , and no more dihedral transitions occur. Their size was characterized by the  $d_{N...N}$  distance as above, and because they are more or less spherical, by their radius of giration  $R_G$ , defined by  $R_G^2 = \sum m_i R_i^2 / \sum m_i$  (where the atom  $i$  of mass  $m_i$  is at a distance  $R_i$  from the center of mass of 222). It depends on the cationic size and charge and on solvation effects for doubly or triply charged ions. For alkali cation cryptates, the size remains similar in water to that in vacuo. From  $Na^+$  to  $Cs^+$ ,  $d_{N...N}$  increases by 0.2 Å and  $R_G$  increases by about 0.10 Å (from 3.96 to 4.10

Å in the gas phase and from 4.00 to 4.10 Å in water). This would lead to an approximate difference of 26.1 cm<sup>3</sup>/mol for the volumes of  $Na^+/222$  and  $K^+/222$  cryptates in water. In water, the average structure is symmetrical and the NC-CO and OC-CO dihedral angles increase from  $Na^+$  to  $Cs^+$  (Table XII), as observed in the solid state<sup>1</sup> and in the optimized structures. The  $Li^+$ ,  $Ca^{2+}$ , and  $Eu^{3+}$  cryptates are distorted and have approximate  $C_2$  symmetry (Table XII). Contrary to what is found for alkali cation complexes, solvation perturbs significantly the size of the  $Ca^{2+}$  and  $Eu^{3+}$  cryptates. As expected, increasing the charge from +1 to +3 with constant size of the cation, from  $Na^+$  to  $Eu^{3+}$ , makes the cryptate more compact:  $d_{N...N}$  decreases from 6.2 to 5.4 Å and  $R_G$  from 3.96 to 3.66 Å. In solution, however,  $d_{N...N}$  decreases by 0.3 Å only and  $R_G$  increases from 4.0 to 4.07 Å. This is because additional coordination of water molecules to the cation induces steric hindrance and deformations of the cage as the cationic charge increases.

There may be also an effect of solvent on the average position of the cations within the cavity (Table VI). We have seen above that, in water, the  $Na^+$ ,  $K^+$ ,  $Rb^+$ , and  $Cs^+$  cations are in inclusive positions, close to the center of mass of 222. This is also true in the gas phase (at about 0.3 Å). The case of  $Li^+$ , too small for 222, is interestingly different. In vacuo,  $Li^+$  undergoes large fluctuations and oscillates between the N and O binding sites, being on the average close to the center of mass. This contrasts with the structure in solution, where  $Li^+$  is in a facial rather than central position because of water attraction (Figure 10). In the  $Na^+$ ,  $Ca^{2+}$ , and  $Eu^{3+}$  series of cryptates, the cations are also on the average close to the center of mass in vacuo (at about 0.2 Å) but tend to move to the solvent in water when the charge increases. Accordingly, the average (center of mass... $M^{**}$ ) distances are respectively 0.5, 0.8, and 1.3 Å (Table VI).

Finally, there are solvent effects on the mobility of the cation itself, as a function of its charge and complementarity with 222 (Table XI).  $Li^+$ ,  $Na^+$ , and  $Ca^{2+}$ , too small for 222, become more mobile in solution than in vacuo, whereas  $K^+$ ,  $Rb^+$ , and  $Cs^+$  become less mobile.  $Eu^{3+}$  displays the lowest mobility in vacuo and in solution, as a result of the strong interactions with oxygen binding sites of 222 and with water.

## Discussion

We have reported theoretical studies on the hydration of a typical neutral ionophore, the 222 macrobicyclic receptor in its free state and in its cation complexes. We gained insight into hydration patterns and energy features of four typical conformers

**Table XII.**  $M^{**}/222$  Cryptates: Average Dihedral Angles

	$Li^+$	$Na^+$	$K^+$	$Rb^+$	$Cs^+$	$Ca^{2+}$ <sup>a</sup>	$Eu^{3+}$ <sup>a</sup>
NC-CO	-64.2	-57.9	-63.5	-68.0	-72.8	61.8	58.5
OC-CO	61.8	58.5	61.7	66.7	72.9	47.9	41.6
CC-OC	-178.5	-177.0	-179.1	-176.6	-175.0	-177.9	-177.6
CC-NC <sup>b</sup>	161.7	162.8	161.5	159.0	157.0	167.6	167.7
CC-NC <sup>b</sup>	-75.1	-72.3	-74.9	-76.8	-77.7	-71.4	-72.9

<sup>a</sup>For  $Ca^{2+}$  and  $Eu^{3+}$ , the structures are similar to K but are deformed and unsymmetrical. There are, for  $Eu^{3+}/222$ , two OC-CO angles at 35° and one at 55° and, for  $Ca^{2+}/222$ , two OC-CO angles at 42° and one at 59°. <sup>b</sup>There are six gauche and six trans CC-NC angles.

of 222 and of  $M^{n+}/222$  cryptates.

The MD method used here permits a study of the dynamics of the solute and of the solvent, which is represented by an "infinite" bath. The energy results depend on the force field representation, particularly on the choice of partial charges. However, as far as relative energies for the same system are concerned, this choice is less critical than for calculating absolute energies.<sup>67</sup> The meaningful thermodynamic quantity is the relative free energy for various conformers involving enthalpy and entropy components. Calculation of this quantity requires very intensive calculations to perform "exhaustive", or at least "representative", conformational sampling in solution, followed by a thermodynamic integration.<sup>19</sup> This is beyond our actual computer resources. For macrocyclic systems, relative free energies of complexation in solution have been calculated,<sup>18,21,68-70</sup> as well as paths for complexation.<sup>20,71</sup> There are also simulations on conformational equilibria for small molecules,<sup>72,73</sup> but to our knowledge, the only one reported so far for macrocyclic receptors is that of Straatsma and McCammon on 18-crown-6.<sup>19</sup> They found that the  $D_{3d}$  conformer has highest population in water, in agreement with Raman studies<sup>74</sup> and with earlier Monte Carlo simulations on typical experimental structures.<sup>49</sup>

**222 Cryptand in Water.** Four conformers of uncomplexed 222, **II**, **OO**, **SS**, and **K**, were selected for this study: **II** is intrinsically the most stable in vacuo, **K** is the only one to have the conformation required for complexation, **OO** and **SS** have diverging heteroatom binding sites. In the gas phase, **K** is calculated to be higher in energy than **II** by about 10 kcal/mol. This value is an upper limit, since lower values are calculated with other force fields (8.0<sup>22</sup> or 1.3 kcal/mol<sup>25</sup>).

In solution, the total internal energy of the system is the sum of the energy of the solute, of the solute-water, and of the water-water interaction energies:  $E_{\text{solute}} + E_{\text{sw}} + E_{\text{ww}}$ . In fact,  $E_{\text{ww}}$  is a larger negative number containing significant fluctuations compared to  $E_{\text{sw}}$  or  $E_{222}$  (Table I). We will in the following assume that  $E_{\text{ww}}$  is similar for the four conformers and consider the  $E_{\text{solute}}$  and  $E_{\text{sw}}$  energies. The relatively small differences in  $E_{\text{sw}}$  for the **II**, **OO**, and **SS** forms (1-7 kcal/mol) contrasts with that of the **K** form ( $\Delta E_{\text{sw}} \approx 30$  kcal/mol), which should more than compensate for the conformational energies. We thus predict that the cryptate-type **K** form of 222 uncomplexed should be significantly better hydrated than **II**, **OO**, and **SS** and have a larger population in water. Whether it corresponds to the absolute energy minimum cannot be predicted solely from the small number of structures considered, but it is likely to be close. One first consequence is that dissolution in water of a crystal of 222 (**II** conformation) should lead to conformational changes. It is noticeable that crystals of free 222 were obtained in dry conditions after successive crystallizations in hexane.<sup>75</sup> Given the high calculated affinity of the **K** form for water and the rigidity of the 222/(H<sub>2</sub>O)<sub>3</sub> framework, it may be speculated that hydrated crystals could be grown, as obtained for polyethers, which bind to neutral molecules,<sup>76</sup> or for the 18-crown-6/water binary system.<sup>77</sup>

**Solvent-Induced Preorganization.** In terms of complexation and ionophoric behavior, it is interesting to find, as for 18-crown-6,<sup>19,49</sup> that, in aqueous solution, the free 222 receptor does not take up

the solid-state conformation, which is not conformationally organized for substrate binding. Instead, our results suggest that water is able to induce conformational changes and to stabilize structures particularly relevant for complexation and transport. Such solvent-induced organization has been also proposed for charged receptors involving polyammonium binding sites.<sup>78</sup> The **K** form provides an example of an "endo-hydrophilic/exo-hydrophobic" structure<sup>64</sup> that displays a relatively high affinity for water. Crown ethers are efficient agents for solubilizing water in chloroform,<sup>79,80</sup> and this might be achieved via strong hydrogen binding of water molecules as characterized for the **K** form of 222, or for the  $D_{3d}$  form of 18-crown-6.<sup>49,81</sup> Interestingly, Raman studies of crown ether and ethers in water show that they adopt conformations similar to those of their cation complexes.<sup>74</sup> Similar solvation pattern may stabilize endo-hydrophilic/exo-hydrophobic forms of other bicyclic cryptands as well involving XCCX units (X = N,O), in conformations organized for complexation and transport.

**Dynamic Behavior.** Many kinetics and NMR experiments have been interpreted on the basis of *in/out* interconversion: temperature-jump studies of proton-transfer reactions,<sup>82</sup> ultrasonic absorption studies,<sup>83</sup> and NMR experiments.<sup>5,12,13</sup> One study of proton transfer reactions has been interpreted instead from an *in-in* predominant conformation.<sup>84</sup> Our previous study on SC24, $nH^+$  and calculations on 222, $nH^+$  support the latter model and favor *in* over *out* protonation.<sup>53,85</sup> There has been much focus on nitrogen inversion at the bridgeheads,<sup>64,86</sup> but other conformational processes such as *in/out* reorientation of oxygens or twisting motions of the molecule have to be considered as well. Interestingly, the lowest frequency mode of vibration of the **K** form (calculated at 40 cm<sup>-1</sup>) corresponds to a twisting motion of  $D_3$  symmetry.<sup>24</sup> Pumping energy into that mode would lead on the path for interconversion from **K** to its mirror image form and account for these kinetics and NMR results.

**Water Coordination or Complexation?** An interesting observation,<sup>75</sup> in the proton NMR spectra of 222, may be reconsidered from our results. Lehn et al. reported that "addition of traces of water to a solution of 222 in CDCl<sub>3</sub> or in hexane does not affect the spectrum of 222 itself, but gives rise to two singlets due to the water protons. One of them, at 4-6 ppm corresponds to the normal resonance of water protons. The other at 2.5-3.0 ppm arises likely from water molecules associated with the macrobicyclic compound".<sup>13</sup> Recent NMR reinvestigations<sup>87</sup> confirm the presence of water bound to 222, in rapid exchange with "free water", in hexane or CDCl<sub>3</sub> solution. We suggest that this particular peak corresponds to an exchange involving water molecules facially hydrogen bonded to 222, as found for the **K** form, rather than from water complexed *inside* the cage.

**Kinetics of Cryptate Formation.** Cryptate formation is characterized by rate constants that are in general abnormally low and considerably less than those calculated on the basis of a simple dissociative interchange mechanism.<sup>88-91</sup> A possible explanation is that the cryptand is not preorganized in solution for complex-

(67) Boudon, S.; Wipff, G. *J. Comput. Chem.* **1990**, *12*, 42-51.  
 (68) Lybrand, T. P.; McCammon, J. A.; Wipff, G. *Proc. Natl. Acad. Sci. U.S.A.* **1986**, *83*, 833-835.  
 (69) Grootenhuis, P. D. J.; Kollman, P. A. *J. Am. Chem. Soc.* **1989**, *111*, 2152-2158.  
 (70) Jorgensen, W. L. *Acc. Chem. Res.* **1989**, *22*, 184-189.  
 (71) van Eerden, J.; Briels, W. J.; Harkema, S.; Feil, D. *Chem. Phys. Lett.* **1989**, *164*, 370-376.  
 (72) Jorgensen, W. L. *J. Phys. Chem.* **1983**, *87*, 5304-5314.  
 (73) Straatsma, T. P.; McCammon, J. A. *J. Chem. Phys.* **1989**, *90*, 3300-3304.  
 (74) Fukushima, K.; Ito, M.; Sakurada, K.; Shiraishi, S. *Chem. Lett.* **1988**, 323-326.  
 (75) Sauvage, J. P. Ph.D. Thesis, Université Louis-Pasteur, 1971.  
 (76) Vögtle, F.; Müller, W. M.; Watson, W. H. *Top. Curr. Chem.* **1984**, *125*, 131-164.  
 (77) Matsuura, H.; Fukuhara, K.; Ikeda, K.; Tachikake, M. *J. Chem. Soc., Chem. Commun.* **1989**, 1814-1816.

(78) Boudon, S.; Decian, A.; Fischer, J.; Hosseini, M. W.; Lehn, J. M.; Wipff, G. *J. Coord. Chem.*, 1991, in press.  
 (79) De Jong, F.; Reinhoudt, D. N.; Smit, C. J. *Tetrahedron Lett.* **1976**, *17*, 1371-1374.  
 (80) De Jong, F.; Reinhoudt, D. N.; Smit, C. J. *Tetrahedron Lett.* **1976**, *17*, 1375-1378.  
 (81) Nordlander, E. H.; Burns, J. H. *Inorg. Chim. Acta* **1986**, *115*, 31-36.  
 (82) Pizer, R. *J. Am. Chem. Soc.* **1978**, *100*, 4239-4241.  
 (83) Schneider, H.; Rauh, S.; Petrucci, S. *J. Phys. Chem.* **1981**, *85*, 2287-2291.  
 (84) Cox, B. G.; Knop, D.; Schneider, H. *J. Am. Chem. Soc.* **1978**, *100*, 6002-6007.  
 (85) Wipff, G.; Wurtz, J. M. *New J. Chem.* **1989**, *13*, 807-820.  
 (86) Simmons, H. E.; Park, C. H. *J. Am. Chem. Soc.* **1968**, *90*, 2428-2432.  
 (87) Kintzinger, J. P. Private communication, 1990.  
 (88) Loyola, V. M.; Wilkins, R. G. *J. Am. Chem. Soc.* **1975**, *97*, 7382-7383.  
 (89) Loyola, V. M.; Pizer, R.; Wilkins, R. G. *J. Am. Chem. Soc.* **1977**, *99*, 7185-7188.  
 (90) Cox, B. G.; Schneider, H. *J. Am. Chem. Soc.* **1977**, *99*, 2809-2811.  
 (91) Bemtgen, J. M.; Springer, M. E.; Loyola, V. M.; Wilkins, R. G.; Taylor, R. W. *Inorg. Chem.* **1984**, *23*, 3348.

ation and that conversion of "nonreactive" to "reactive" conformers has to be achieved prior to or during the complexation.<sup>23</sup> This is not supported by our results. We suggest instead that solvent effects play a major role in stabilizing a form suitable for complexation through a specific hydrogen-bonding pattern. Complexation of a cation into such a form requires dehydration, not only of the cation, but also of the receptor. Such a process should be more difficult for bicyclic receptors than for open monocyclic ones, due to topological features and to the related hydration pattern. This explanation is supported by the fact that the enthalpy of transfer for 222 from water to methanol is large and positive (13.9 kcal/mol).<sup>92</sup> Our results make it clear that such a stable and unique solvation pattern as found for the K form cannot be achieved by methanol.

**Structure of Solvent and Conformation of the Cryptand. On the Importance of Bridging Water Structures.** We have discussed the hydration of the K form in more detail than that of II, OO, and SS, because no clear pattern was found for the latter, which have poorer hydration. Comparison of these forms is reminiscent of what was found for 18-crown-6, where bridging water molecules make particularly stable arrangements over  $D_{3d}$  and  $C_1$  conformers.<sup>49</sup> This contrasted with the  $C_i$  form, which made only linear and weak hydrogen bonds with water and had the weakest hydration energy. The hydration energy did not follow the coordination number of the heteroatoms of the crown, which was largest for the weakly hydrated  $C_i$  form. For the II, OO, and SS forms of 222, there are more water molecules involved in hydrogen bonds with the solute than for the K form (Table II), but because of topological features, they can make only linear rather than bridging hydrogen bonds. It therefore appears, as confirmed by related solid-state structures<sup>76,81</sup> and recent theoretical work,<sup>93</sup> that bridging water molecules provide a particularly stable hydration pattern, forming a "supermolecule"<sup>47</sup> with the solute. It has been proposed that cyclic ligands might be less well solvated than linear or (poly)cyclic ones, due to steric hindrance in the more compact ring structure.<sup>94</sup> Our results question somewhat this view, since bridging solvation is more compatible with cyclic than acyclic topologies of the solute.

More generally, these studies show that solute-solvent interaction energies cannot be predicted simply from the surface of heteroatoms accessible to the solvent, due to solvent granularity. Such an additive scheme for estimating free energies of hydration as used for proteins<sup>95</sup> is not valid for these macrocyclic compounds, due to possible cooperative binding in some of the conformers.

**222 Cryptates in Water. Can the Anion be Neglected?** Our simulations of cryptates in water were performed assuming that there are no cation-anion interactions at short or medium distances, and no anion was taken into account explicitly. This is a simplification since, depending on the solvent, such interactions may occur. For instance, in ethereal (DME, THF, MTHF, DMTHF) or aromatic solvents,  $\text{Na}^+$  cryptates of 222 can form with the 9-fluorenone anion radical both contact-type and cryptand-separated ion pairs.<sup>96</sup> The equilibrium between ion pairs results from complex effects such as the stability of the cryptate, the nature of the uncomplexed ion pair in solution, and the possible interactions of the "naked" anion with the solvent. Anion solvation is more effective by water than by ethers or aromatic solvents and should favor separated cryptate-anion pairs. To our knowledge, there has been no experimental proof for contact-type ion pairs involving cryptates of 222 in water (cryptate formation is rather used to activate the reactivity of the associated anion<sup>97</sup>).

**Cation-Water Interactions.** As far as solvent coordination to the complexed cations is concerned, significant shielding may be

anticipated for polycyclic ligands like 222 compared to monocyclic ligands such as 18-crown-6<sup>9</sup> or polyamines.<sup>98,99</sup> Our simulations reveal that shielding is not totally effective and that there are cation-solvent interactions that are cation dependent. For the highly charged  $\text{Ca}^{2+}$  or  $\text{Eu}^{3+}$  cryptates, these results are consistent with solid-state structures, in which the cation is coordinated either to one water molecule (in  $\text{CaBr}_2 \cdot 3\text{H}_2\text{O}/222$ )<sup>100</sup> or to oxygen atoms of counteranions (in  $\text{Eu}^{3+} \cdot \text{ClO}_4^-/222$ ).<sup>39-41</sup> In the  $\text{Pb}(\text{SCN})_2/222$  and  $\text{Ba}(\text{NCS})_2 \cdot \text{H}_2\text{O}/222$  cryptates,  $\text{Pb}^{2+}$  and  $\text{Ba}^{2+}$  are coordinated respectively to two  $\text{SCN}^-$  and to  $\text{H}_2\text{O}$  and one  $\text{NCS}^-$ .<sup>1,101</sup> There is an interesting structure of the  $\text{K}^+/222$  cryptate, in which  $\text{K}^+$  has a nine coordination, being at 3.16 Å from a nitrosyl oxygen.<sup>102</sup> For alkali cation cryptates, however, no water coordination is found in the solid-state structures,<sup>1</sup> the  $\text{Na}^+$ ,  $\text{K}^+$ ,  $\text{Rb}^+$ , and  $\text{Cs}^+$  cations being at the center of the cage, coordinated to the ligand only. In solution either, there is to our knowledge no direct proof of water coordination to alkali cations complexed by 222. Far-infrared and Raman studies of  $\text{Li}^+$  and  $\text{Na}^+/222$  cryptates in nitromethane, pyridine, and acetonitrile seem rather to indicate that these ions are completely enclosed in the cavity.<sup>103</sup> This technique may however not be sensitive enough to draw firm conclusions. NMR studies on  $^{133}\text{Cs}^+/222$  inclusive cryptates in methanol, acetone, propylene carbonate, and *N,N*-dimethylformamide solutions show that, at low temperature, the  $^{133}\text{Cs}$  chemical shift of the complexed cation becomes completely independent of the solvent,<sup>5</sup> suggesting therefore no significant interactions between  $\text{Cs}^+$  and these solvents. It is not clear whether this conclusion can be extended to water.

Indirect evidence for solvent interactions with the complexed cation comes from thermodynamic results on transfer equilibria for  $\text{M}^+/222$  cryptates from water to methanol. Contrary to previous assumptions on the constancy of the  $\Delta H_t^\circ$ ,  $\Delta G_t^\circ$ , and  $\Delta S_t^\circ$  values for  $\text{M}^+/222$ , Abraham et al. found considerable variations with  $\text{M}^+$  and concluded that  $\text{M}^+$  is not completely prevented from interacting with the solvent.<sup>92</sup>

Cryptate-water interactions may contribute to the entropies of ligation  $\Delta S_l$  as defined by Lehn et al.<sup>65</sup> for the hypothetical reaction



The constancy of  $\Delta S_l$  for  $\text{Na}^+$ ,  $\text{K}^+$ , and  $\text{Rb}^+$  in water led first to the conclusion that the  $\text{M}^+$  cation in ( $\text{M}^+/222$ ) is unhydrated. More recent determinations confirm this result for certain ions but find exceptions such as  $\text{Cs}^+$  and  $\text{Ag}^+$  in water and  $\text{Li}^+$  and  $\text{Ag}^+$  in methanol.<sup>92</sup> For the series of divalent cations  $\text{Ca}^{2+}$ ,  $\text{Sr}^{2+}$ , and  $\text{Ba}^{2+}$ , there are also differences in  $\Delta S_l$ , which may be related to a change in hydration pattern.<sup>65</sup>

Volumes of complexation of  $\text{M}^+$  and  $\text{M}^{2+}/222$  cryptates in water and in methanol have been reported.<sup>104,105</sup> They are not easy to interpret since they may result from the solute itself as well as from changes in solvation pattern. From these studies, Morel et al. concluded that the ligand does not shield totally the trapped cation from the environment and that the inclusive cryptate behaves more like a charged species than like the neutral ligand.

For lanthanide  $\text{L}^{3+}$  cryptates, there are quantitative estimates of water coordination to  $\text{L}^{3+}$  from spectroscopic observations. For  $\text{Eu}^{3+}/222$  cryptates, a somewhat larger solvent coordination is expected, given the poorer steric fit between the cage and the cation, compared to  $\text{Eu}^{3+}/221$ . There are similar interactions in

(98) Hannongbua, S. V.; Rode, B. M. *J. Sci. Soc. Thailand, J.* **1985**, *11*, 135-139.

(99) Ruangpornvisuti, V. W.; Probst, M. M.; Rode, B. M. *Inorg. Chim. Acta* **1987**, *134*, 297-302.

(100) Metz, B.; Moras, D.; Weiss, R. *Acta Crystallogr.* **1973**, *B29*, 1377-1382.

(101) Metz, B.; Weiss, R. *Inorg. Chem.* **1974**, *13*, 2094-2099.

(102) Chu, C. T. W.; Lo, F. Y. K.; Dahl, L. F. *J. Am. Chem. Soc.* **1982**, *104*, 3409-3422.

(103) Cahen, Y. M.; Popov, A. I. *J. Solution Chem.* **1975**, *4*, 599-607.

(104) Morel-Desrosiers, N.; Morel, J. P. *New J. Chem.* **1979**, *3*, 539-543.

(105) Morel-Desrosiers, N.; Morel, J. P. *J. Am. Chem. Soc.* **1981**, *103*, 4743-4746.

(92) Abraham, M. H.; Danil De Namor, A. F.; Schulz, R. A. *J. Chem. Soc., Faraday Trans. 1* **1980**, *76*, 869-884.

(93) Ben-Naim, A. *Biopolymers* **1990**, *29*, 567-596.

(94) Hinz, F. P.; Margerum, D. W. *J. Am. Chem. Soc.* **1974**, *96*, 4993-4994.

(95) Kang, Y. E.; Gibbs, K. D.; Némethy, G.; Sheraga, H. A. *J. Phys. Chem.* **1988**, *92*, 4739-4742.

(96) Nakamura, K. *J. Am. Chem. Soc.* **1980**, *102*, 7846-7848.

(97) Lehn, J. M. *Pure Appl. Chem.* **1980**, *52*, 2303-2319.

the  $\text{Eu}^{2+}/221$  and  $\text{Eu}^{2+}/222$  cryptates<sup>106</sup> consistent with our results on divalent cryptates. The anions used in those experiments are big enough to prevent significant ion pairing with the complexed cation, unlike small anions such as  $\text{F}^-$ .<sup>66,107</sup> There is therefore satisfactory agreement between our calculated 3.9 water coordination in  $\text{Eu}^{3+}/222$  and the experimental 3.2 value in the  $\text{Eu}^{3+}/221$  cryptate.

In addition to direct water-ion coordination, we find that water is structured beyond the first sphere of coordination due to long-range electrostatic effects, especially for highly charged ions. Upon complexation, the water dipoles for interfacial water molecules in the second coordination sphere are reversed. These results are also consistent with the fact that entropies of ligation  $\Delta S_1$  are more negative for  $\text{M}^{2+}$  than for  $\text{M}^+$  cations (about -33 and -50 eu, respectively).<sup>65</sup> It is thus understandable that transfer of these cryptates from water to a nonaqueous solvent is more difficult than for alkali cation cryptates,<sup>15</sup> despite the fact that cryptates are usually depicted as big hydrophobic cations.<sup>65,92,104,105</sup>

**Partition Coefficients of Cryptands and Cryptates and Transport Properties. What Makes Water Unique?** Solvent-cryptate and solvent-cryptand interactions for nonaqueous solvents are weak in comparison with the cation-solvent ones since the former do not vary significantly from one solvent to the other. The difference in the free energies or enthalpies of transfer from water to aprotic nonaqueous solvents (DMF, PC, AN, and DMSO) between 222 cryptates and the 222 cryptand have been found indeed to be quite constant.<sup>108</sup> There is also a linear correlation between entropies of complexation and entropies of solvation of  $\text{M}^+$  cations for solvents such as MeOH, PC, DMF, DMSO, and  $\text{MeNO}_2$ ,<sup>109</sup> but again water does not fit in the series and seems to give particular interactions. The entropy of 222 cryptate formations in water is more favored by ca. 19 cal  $\text{K}^{-1} \text{mol}^{-1}$  with respect to that found in the other solvents.<sup>109</sup> We suggest that water is unique compared to the solvents in which these experiments have been carried out because, in addition to its small size and self-association properties,<sup>110</sup> it solvates significantly both the cryptand (via  $H_w$  protons) and the cryptate (via  $O_w$  direct coordination to the cation and longer range interactions). This particular hydration of the cryptand is consistent with its large positive enthalpy of transfer from water to methanol (13.9 kcal/mol) compared to that of cryptates (5.5 to 3.9 kcal/mol from  $\text{Na}^+$  to  $\text{Cs}^+$ ) and with the corresponding large change in entropy for the cryptand (42.9 cal  $\text{K}^{-1} \text{mol}^{-1}$ ), compared to cryptates (26.0–15.1 cal  $\text{K}^{-1} \text{mol}^{-1}$  from  $\text{Na}^+$  to  $\text{Cs}^+$ ). From our results, it appears that the kind of solvation pattern found for the K form of the cryptand (via the  $H_w$  protons) cannot be achieved by most of the nonaqueous solvents nor by methanol. On the other hand, for the cryptates, partial coordination of the complexed cation to any of these solvents, similar to that found here, may still take place. This is supported by simulations of cryptates in methanol.<sup>51,121</sup>

For the 221 cryptand, a smaller analogue of 222, NMR and calorimetric studies on  $\text{Na}^+$  and  $\text{K}^+$  complexation in nonaqueous

solvents led Popov et al. to conclude that "in certain solvents there is a specific solvent-221 interaction that affects the configuration of the free ligand and undoubtedly influences its complexation ability with alkali metal and other cations. It is evident, therefore, that the mechanism and kinetics of macrocyclic complex formation in various solvents are strongly influenced not only by cation-solvent but, at least in certain media, by ligand-solvent interactions".<sup>10</sup> Our present results support fully this conclusion.

One consequence of these hydration effects concerning transport experiments<sup>15,111,112</sup> is that when such a carrier as 222 diffuses from an aqueous to a nonaqueous solution like chloroform, either in its free or complexed state, some water molecules should remain firmly bound to the carrier and follow from one phase to the other. This could be checked by appropriate labeling experiments.

Following the solvation pattern found in water, one can speculate that other protic solvents such as primary amines or liquid ammonia<sup>113,114</sup> should behave somewhat like water in solvating both the bicyclic cryptands and cryptates. Their  $-\text{NH}_2$  moiety may be doubly hydrogen bonded to the cryptands like water in interbridging positions of the K form and interact with the cation of the cryptates as well. Primary amides might interact similarly with the cryptands via their  $-\text{NH}_2$  hydrogens and with the encapsulated cation of cryptates via their carbonyl oxygen.

To conclude, we have gained microscopic insights on a very efficient neutral ionophore in water, in its free and complexed states. The results allow for reinterpretation of several experimental facts including spectroscopic, thermodynamic and transport properties. Suggestions have been made for experiments to be performed. Solvation effects are known to determine conformational equilibria,<sup>72</sup> and conformations of molecules such as peptidic nucleic acid derivatives (see for instance refs 115–117 and references cited therein). Our study demonstrates the importance of solvent-solute interactions on conformation and recognition properties of macrocyclic receptors and more generally on molecular recognition.<sup>2,3,118,119</sup>

**Acknowledgment.** We thank Prof. J.-M. Lehn, A. I. Popov, and Dr. J.-P. Kintzinger for stimulating discussions. The CNRS-IBM Scientific Group for Molecular Modelling and the CNRS Computer Center of Strasbourg Cronenbourg have provided the computer means for this study and are acknowledged. P.A. is also grateful to the French Ministry of Research for providing a grant. G.W. is grateful to the Région Alsace and to the Biostructure company for funding a computer graphics workstation.

- 
- (111) Pressman, B. C. *Annu. Rev. Biochem.* **1976**, *45*, 501–530.  
 (112) Lamb, J. D.; Christensen, J. J.; Oscarson, J. L.; Nielsen, B. L.; Asay, B. W.; Izatt, R. M. *J. Am. Chem. Soc.* **1980**, *102*, 6820–6824.  
 (113) Gans, P.; Gill, J. B.; Towner, J. N. *J.C.S. Dalton* **1977**, 2202–2204.  
 (114) Dye, J. L.; DeBaker, M. G. *Annu. Rev. Phys. Chem.* **1987**, *38*, 271–301.  
 (115) Baker, E. N.; Hubbard, R. E. *Prog. Biophys. Mol. Biol.* **1984**, *44*, 97–179.  
 (116) Wüthrich, K. *NMR of Proteins and Nucleic Acids*; Wiley & Sons: New York, 1986.  
 (117) Kessler, H.; Griesinger, C.; Lautz, J.; Müller, A.; van Gunsteren, W. F.; Berendsen, H. J. C. *J. Am. Chem. Soc.* **1988**, *110*, 3393.  
 (118) Diederich, F. *Angew. Chem., Int. Ed. Engl.* **1988**, *27*, 362–386.  
 (119) Smithrud, D. B.; Diederich, F. *J. Am. Chem. Soc.* **1990**, *112*, 339–343.  
 (120) Auffinger, P.; Wipff, G. *J. Inclusion Phenom.* **1991**, in press.  
 (121) Auffinger, P.; Wipff, G. *Advances in Biomolecular Simulations. J. Chim. Phys. Phys.-Chim. Biol.* **1991**, in press.

(106) Sabbatini, N.; Dellonte, S.; Ciano, M.; Bonazzi, A.; Balzani, V. *Chem. Phys. Lett.* **1984**, *107*, 212.

(107) Sabbatini, N.; Perathoner, S.; Lattanzi, G.; Dellonte, S.; Balzani, V. *J. Phys. Chem.* **1987**, *91*, 6136–6139.

(108) Gutknecht, J.; Schneider, H.; Stroka, J. *Inorg. Chem.* **1978**, *17*, 3326–3329.

(109) Danil de Namor, A. F. *J. Chem. Soc., Faraday Trans. 1* **1988**, *84*, 2441–2444.

(110) Franks, F. In *Water: A Comprehensive Treatise*; Franks, F., Ed.; Plenum Press: New York, 1973.